International
Progress Report

IPR-05-21

Äspö Hard Rock Laboratory

Äspö Pillar Stability Experiment

Hydromechanical data acquisition experiment at the APSE site

Diego Mas Ivars

Itasca Geomekanik AB

February 2005

Svensk Kärnbränslehantering AB
Swedish Nuclear Fuel
and Waste Management Co
Box 5864
SE-102 40 Stockholm Sweden
Tel 08-459 84 00
+46 8 459 84 00
Fax 08-661 57 19
+46 8 661 57 19

Äspö Hard Rock
Laboratory

Report no.	No.
IPR-05-21	F86K
Author	Date
Diego Mas Ivars	February 2005
Checked by	Date
Rolf Christiansson	2005-10-17
Approved	Date
Anders Sjöland	2005-11-08

Äspö Hard Rock Laboratory

Äspö Pillar Stability Experiment

Hydromechanical data acquisition experiment at the APSE site

Diego Mas Ivars

Itasca Geomekanik AB

February 2005

Keywords: Äspö Pillar Stability Experiment, De-stressing, Inflow, Fracture aperture, Fracture normal displacement, Fracture shear displacement, Hydro Monitoring System, Coupled stress-flow behaviour

Abstract

In this project a large field experiment has been conducted with the aim of acquiring hydro-mechanical data during the drilling of the de-stressing slot at the APSE site. The de-stressing of the pillar was expected to cause a number of coupled hydro-mechanical effects in two NW-SE striking sub-vertical conductive fractures intersecting the deposition hole size borehole DQ0066G01. The effective normal stress acting on the conductive fractures was expected to change with the consequent influence in inflow. Besides, the change in normal stress would affect the fracture shear strength, which, combined with the change in shear stress along the fracture, could lead to slip and dilation of the fracture. Therefore, fracture displacements, fracture inflow and total inflow into the deposition hole size borehole (DQ0066G01) have been monitored during the drilling of the de-stressing slot.

Fracture normal displacements (opening) of up to 0.6 mm and shear displacements of up to 0.9 mm have been registered during the drilling of the slot. The inflow coming from fracture 08 increased from 2.4 l/min to 4 l/min and the inflow from fracture 14 increased from 6.1 l/min to 18 l/min. Before the drilling of the slot the water inflow from the two sub-vertical fractures monitored accounted for 60% of the total inflow into the hole. After the drilling of the slot the inflow coming from these two fractures was 72 % of the total inflow.

Several boreholes in the HMS system (Hydro Monitoring System) were selected to assess the influence of the de-stressing slot on the water pressure response on other locations at the Äspö HRL. Strong responses were found in boreholes KA3385A, KA3386A01 and KA2598A and a weak response was also registered in borehole KI0025F.

Sammanfattning

I projektet har ett fälttest utförts i syfte att insamla hydro-mekaniska data under borrningen av en avlastningsslits i APSE-tunneln. Avlastningen av pelaren mellan två borrhål, stora som deponeringshål, förväntades ge flera kopplade hydromekaniska effekter hos två NW-SE strykande subvertikala vattenförande sprickor som korsar det ena borrhålet (DQ0066G01). Effektivspänningen över sprickorna förväntades ändras och därmed ge en inverkan på vatteninflödet till borrhålet. Dessutom förväntades förändringen i normalspänning att ge en motsvarande förändring i skjuvhållfasthet, vilket i kombination med förändringen i skjuvspänning längs sprickan kunde leda till skjuvbrott och dilatation. Därför uppmättes rörelserna och inflödet från dessa två sprickor samt det totala inflödet till borrhålet under borrningen av avlastningsslitsen.

Normalrörelser över sprickorna (öppning) upp till 0.6 mm och skjuvrörelser upp till 0.9 mm har observerats under borrningen av avlastningsslitsen. Mätningarna på de enskilda sprickorna visade att inflödet från spricka 08 hade ökat från 2.4 l/min till 4 l/min och inflödet från spricka 14 ökat från 6.1 l/min till 18 l/min. Före borrningen av slitsen utgjorde inflödet från dessa två sprickor 60% av det totala inflödet till hålet, och efter borrningen av slitsen var inflödet från dessa två sprickor 72% av det totala inflödet.

Flera borrhål i HMS-systemet (Hydro Monitoring System) valdes ut för att studera responsen av slitsen på vattentrycket i laboratorieområdet. Stark respons sågs i borrhålen KA3385A, KA3386A01 och KA2598A och en svag respons registrerades också i K10025F.

Contents

1 Introduction

One of the recent experiments performed by SKB at the Äspö HRL has been the Äspö Pillar Stability Experiment (APSE). This experiment was designed to demonstrate the capability to predict spalling in a fractured rock mass, considering the effect of backfill on the rock mass response, and to compare the mechanical and thermal capabilities of 2D and 3D numerical models. To achieve spalling, high stresses were induced by the choice of tunnel geometry and by boring two vertical boreholes of deposition hole size close to each other (Figure 1-1). By using this geometrical configuration the stress level in the pillar between the two holes reached high values, but not high enough to initiate spalling. To further increase the stress the rock volume between the boreholes was heated. The effect of the confining pressure was also studied by applying a uniform pressure of 0.8 MPa to the wall of the first hole drilled. The pressure was maintained during the drilling of the second hole and the heating phase. After the heating, the pressure was stepwise reduced while the response of the rock mass was monitored by acoustic emission /Andersson, 2004a/.

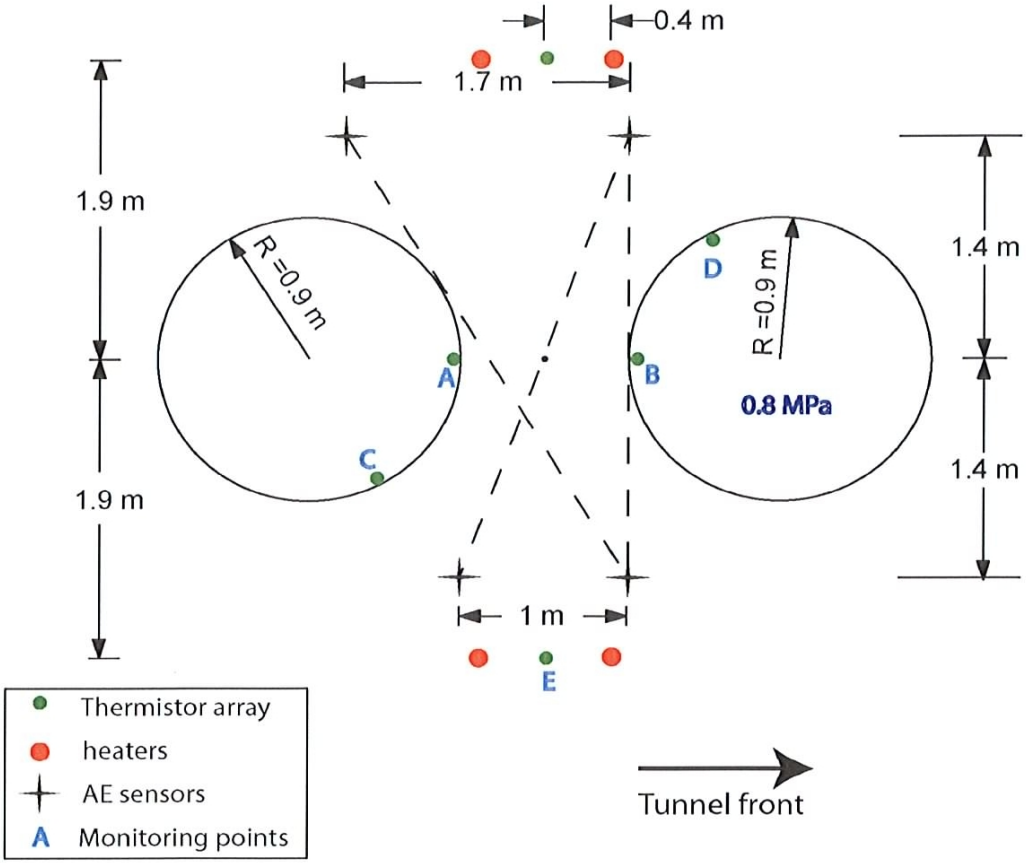

Figure 1-1. *Layout of the APSE project geometry /Andersson, 2004a/.*

One of the last phases of the APSE project involved the extraction of the pillar to study the effect of the high stress concentration obtained during the experiment. Before cutting and extracting the pillar it had to be previously de-stressed. The de-stressing of the pillar was carried out by drilling a semicircular array of boreholes (Figure 1-2).

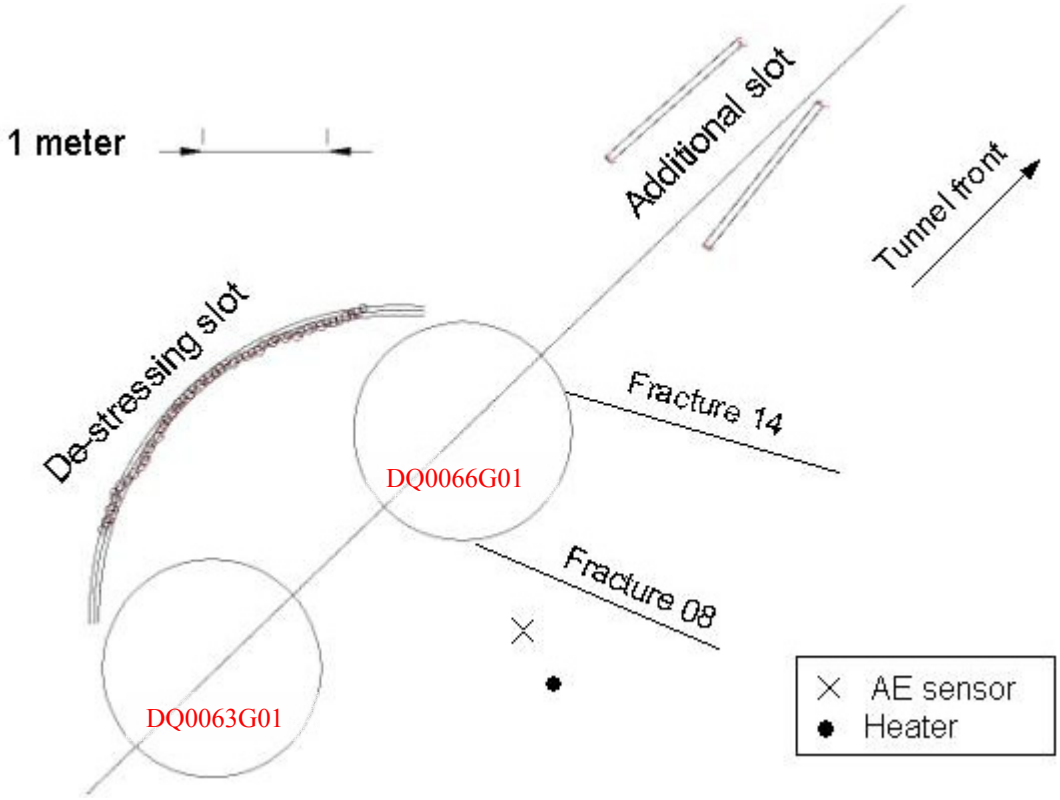

Figure 1-2. *Layout of the HM data acquisition experiment. The AE sensor and heater boreholes in the scheme intersect fracture 08 at 5 m and 6.15 m depth respectively.*

The Hydro-Mechanical Data Acquisition Experiment has been conceived due to the fact that when drilling the first of the two vertical holes for the Äspö Pillar Stability Experiment, two highly conductive sub-vertical fractures were intersected and the water inflow into the excavation reached a value of around 30 l/min. It was expected that the de-stressing of the pillar could cause a number of coupled hydro-mechanical effects in both sub-vertical fractures. The effective normal stress acting on the conductive fractures was expected to change with the consequent influence in inflow. Besides, the change in normal stress would affect the fracture shear strength, which, combined with the change in shear stress along the fracture, could lead to slip and dilation of the fracture. For this reason it was decided to monitor the inflow and the fracture displacements for the duration of the de-stressing work. Pore pressure changes would also be followed in further locations expected to be influenced by the de-stressing of the pillar, making use of the existing HMS (Hydro Monitoring System) at the Äspö HRL.

1.1 Background

In the nuclear waste disposal programs the criteria for the acceptance/rejection of emplacements of emplacements of the deposition holes following the KBS-3 concept will depend on the expected consequences of a number of long and short-term processes. One of the criteria for this acceptance/rejection is related to the inflow into the open deposition hole during emplacement of the waste canisters.

The ability to predict inflow is of importance for several aspects, such as:

- Evaluation of experimental results in the Äspö HRL. A good understanding of the mechanisms controlling inflow would improve the possibilities for good experimental set-ups and accurate result interpretation.

- Evaluation and comparisons between potential repository sites. It is desirable to be able to predict the inflow conditions into the excavations, already before the construction work starts, based on hydraulic measurements made in small diameter bore holes.

- Evaluation of the expected bentonite buffer behaviour. The amount of inflow into deposition holes will influence the time needed for saturation and also the expected performance of the buffer.

- Design and optimisation of the repository layout. Poor prediction of inflow could lead to less optimal design alternatives.

Due to the complexity involved in the processes influencing the inflow into excavations (stress-permeability coupling, groundwater degassing, bubble trapping, possible turbulence effects, temperature effects, etc), SKB has conducted in recent years a number of large field tests where prediction of inflow into tunnels or depositions holes has been a component:

- the Site Characterisation and Validation Test in Stripa /Olsson, 1992/,

- the Prototype Repository Test /Rhén and Forsmark, 2001/,

- and the Groundwater Degassing and Two-Phase Flow experiments /Jarsjö et al, 2001/ in Äspö HRL.

The present project has been designed to provide a valuable source of data to improve the understanding about inflow into excavation, and specially about stress-permeability coupling, which is one of the most relevant processes governing the inflow into hard rock excavations /Mas Ivars, 2004/.

1.2 Geological overview and in-situ conditions

A complete and detailed geological description of the tunnel TASQ can be found in /Staub et al, 2004; Magnor, 2004 and Staub et al, 2003/. According to these reports, the geology and rock mechanics properties in the tunnel TASQ area are similar to those found elsewhere in the 450 m level of the Äspö HRL (Figure 1-3). The only exception to this similarity is a heavily oxidized, brittle-ductile shear zone striking along the TASQ-tunnel and dipping southeast (Figure 1-4). There is no crush zone or open fractures associated to the shear zone which appears quite old and sealed. However, the strength of the rock in the shear zone is considerably lower than that of fresh Äspö diorite and it could start to yield and the induced deformation could cause a re-distribution of stresses that would reduce the possibility of spalling. The final assessment about the influence of the shear zone on the APSE experiment concluded that the presence of this feature would not endanger the outcome of the experiment.

Table 1-1 shows the characteristics of the modeled shear zone.

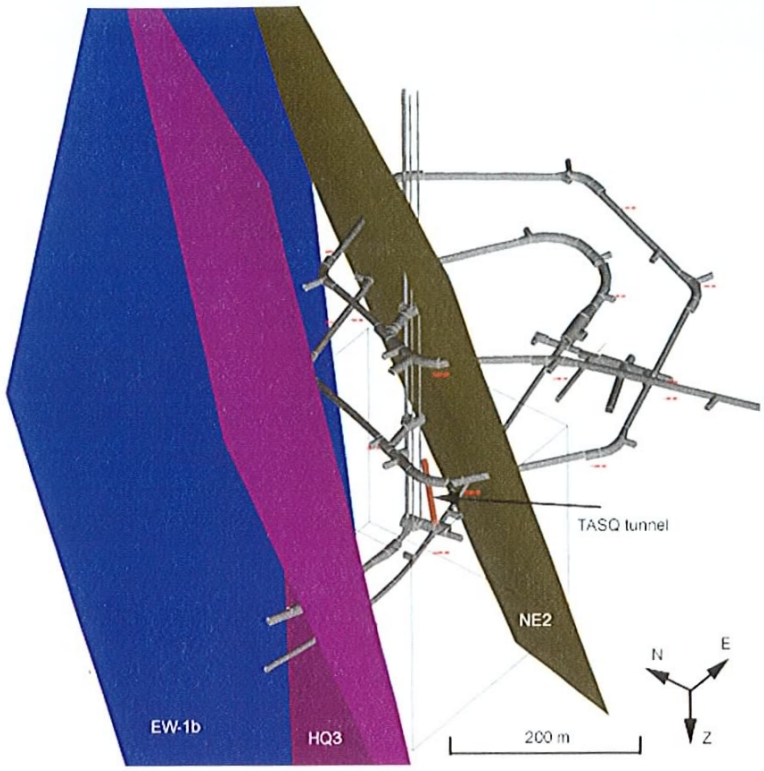

Figure 1-3. *Location of the TASQ tunnel and the major identified structures around it in the Äspö HRL /Staub et al, 2004/.*

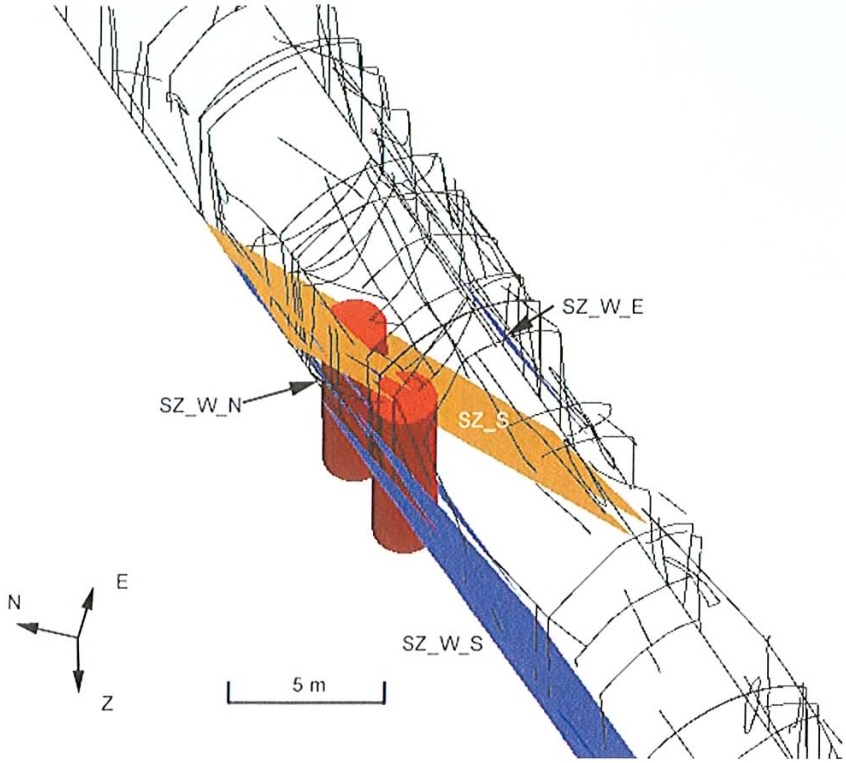

Figure 1-4. *3D visualization of the shear zone. The red cylinders are a visualization of the large holes /Staub et al, 2004/.*

Table 1-1. Characteristics of the modelled shear zone /Staub et al, 2004/.

	Strike (°)	Dip (°)	Remarks
SZ_W_S	33.3	68	Main part of the SZ_W branch, based on observations on the wall and boreholes
SZ_W_E			Displaced section, based on the fracture between Ch 59 and 64 m.
SZ_W_N			Northern part of the SZ_W branch based on the fracture 7, Ch 64-69 m.
SZ_S	23.6	56.2	

1.2.1 Sub-vertical structures

A number of sub-vertical structures have been identified in the experiment volume (Figure 1-5). Sub-vertical fracture 14 as presented in Figure 1-2 is not included in the figure and fracture 08 in Figure 1-2 is fract_1 in Figure 1-5.

Table 1-2 presents the estimated orientation of the sub-vertical structures in the APSE volume.

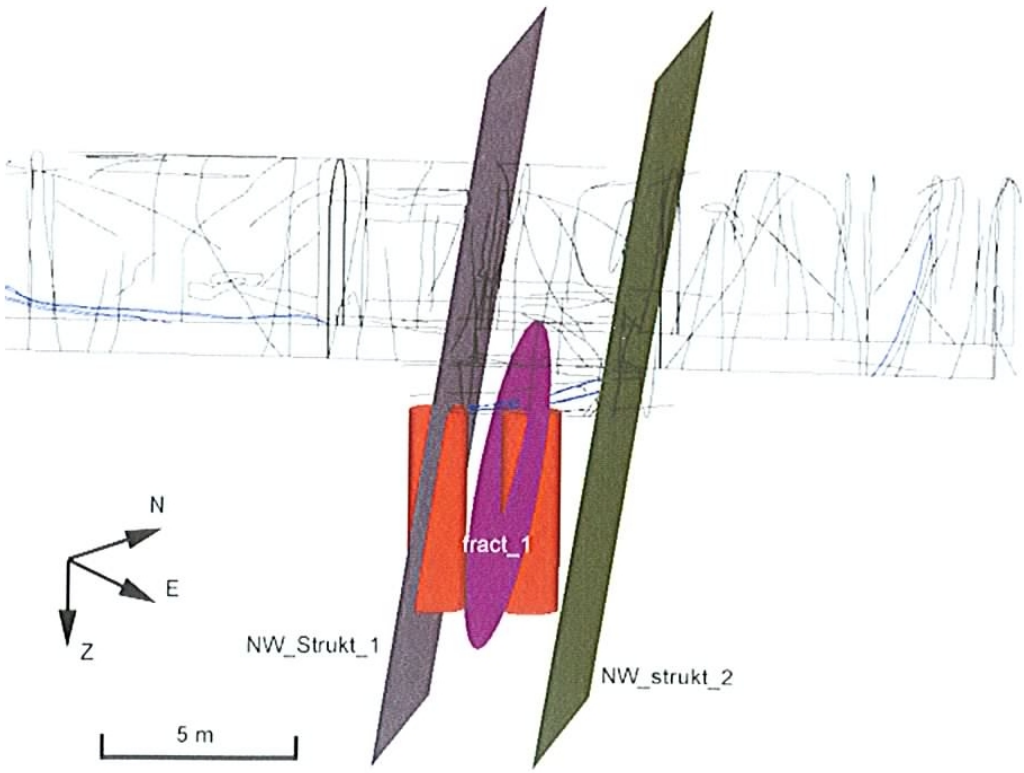

Figure 1-5. *Interpreted sub-vertical structures in the experiment volume. fract_1 refers to fracture 08 (Figure 1-2) as presented in this report. The red cylinders are a visualization of the large holes /Staub et al, 2004/.*

Table 1-2. Orientation of the sub-vertical structures in the APSE volume.

	Strike (°)	Dip (°)
Fracture 08	112	80
Fracture 14	106	76
NW_struct_1	126.9	81.3
NW_struct_2	126.7	80.8

1.2.2 Sub-horizontal structures

Two sub-horizontal features have been observed in most of the boreholes mapped in the area. From these observations, two distinct features have been identified and modeled as a wide breccia and a thinner epidote filled fractures (Figure 1-6).

The orientation of the interpreted sub-horizontal structures can be found in Table 1-3.

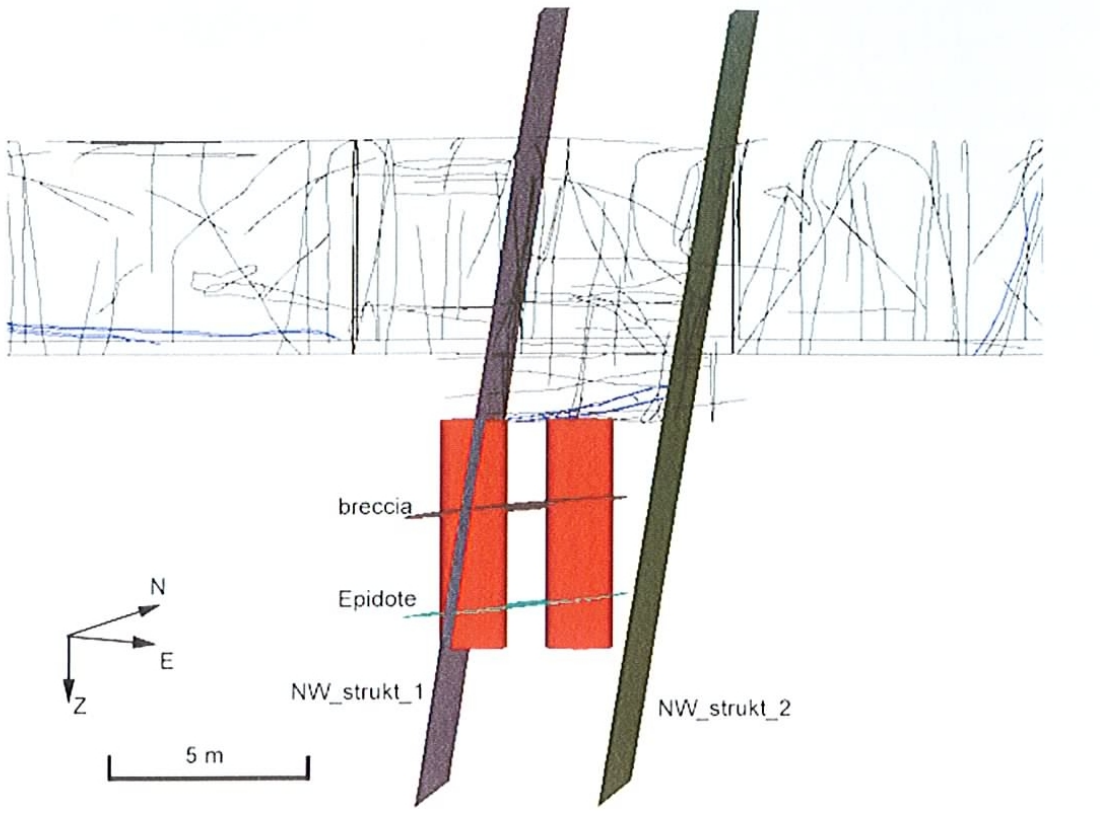

Figure 1-6. *Interpreted "breccia" and "epidote" structures in the APSE area. The red cylinders are a visualization of the large holes /Staub et al, 2004/.*

Table 1-3. Orientation of the sub-horizontal structures in the APSE volume.

	Strike (°)	Dip (°)
"Breccia" filled fracture	170.4	7.5
"Epidote" filled fracture	140.3	6.1

1.2.3 In-situ stress

The in-situ stress tensor used in the modelling exercises reported in /Andersson, 2004a; Fredriksson et al, 2004; Rinne et al, 2004 and Wanne et al, 2004/ was derived from a compilation of available rock stress measurements in the vicinity of the experiment volume (Table 1-4).

Table 1-4. Stress tensor used for the numerical modelling using a Young's modulus of 55 GPa.

	Magnitude (MPa)	Trend/Plunge (degrees)
Sigma 1	27	310/07
Sigma 2	15	090/83
Sigma 3	10	208/00

The stress estimation was later refined using results from convergence measurements made during the excavation of the TASQ tunnel. The resulting refined stress tensor is shown in Table 1-5. As reported in /Andersson, 2004a/, if scooping calculations are made with 3D models using these two slightly different stress tensors in Table 1-4 and Table 1-5, the difference is small. It was therefore decided not to re-run the numerical models using the final stress tensor derived from the back analysis.

Table 1-5. Final stress tensor derived by back calculation of the convergence measurements using a Young's modulus of 55 GPa.

	Magnitude (MPa)	Trend/Plunge (degrees)
Sigma 1	30	310/00
Sigma 2	15	090/90
Sigma 3	10	208/00

1.2.4 Mechanical and thermal properties

Table 1-6 and Table 1-7 show the rock mechanical parameters derived during the characterization process and used as input data for the numerical models of the APSE project.

Table 1-6. Mechanical and thermal properties of intact Äspö diorite used in the numerical models of the APSE project.

Parameter	Value	Unit
Uniaxial compressive strength, low	130	MPa
Uniaxial compressive strength, high	210	MPa
Young's modulus, intact rock	76	GPa
Young's modulus, rock mass	55	GPa
Poisson's ratio, intact rock	0.25	-
Poisson's ratio, rock mass	0.26	-
Friction angle, intact rock	49	Degrees
Friction angle, rock mass	41	Degrees
Cohesion, intact rock	31	MPa
Cohesion, rock mass	16.4	MPa
Tensile strength	14.3	MPa
Thermal conductivity	2.60	W/m°C
Volume heat capacity	2.10	MJ/m^3°C
Linear expansion coefficient	7.0E-06	1/°C
Specific heat	775	J/kg°C
Density	2.731	g/cm^3
Initial temperature of the rock mass	15	°C
Crack initiation stress	121	MPa
Crack damage stress	204	MPa

Table 1-7. Mechanical fracture properties used in the numerical models.

Parameter	Value	Unit
Normal stiffness, sub-vertical fractures	61.5	GPa/m
Normal stiffness, sub-horizontal fractures	21,9	GPa/m
Shear stiffness, sub-vertical fractures	35.5	GPa/m
Shear stiffness, sub-horizontal fractures	15.7	GPa/m
Residual friction angle, sub-vertical fractures	31	Degrees
Residual friction angle, sub-horizontal fractures	30	Degrees
Dilation angle	2.3	Degrees
Mode I toughness, K_{IC}	3.8 ± 0.1	$MPa/m^{1/2}$
Mode II toughness, K_{IIC}	4.4 to 13.5	$MPa/m^{1/2}$
Initial normal fracture stiffness (Force 0-1.5 kN)), NW-struct_1 (Figure 1-5)	175 ± 68	GPa/m
Normal stiffness (Force (12-25 kN)), NW-struct_1 (Figure 1-5)	26976 ± 22757	GPa/m

1.2.5 Water

As reported in /Magnor, 2004/, leakage in the TASQ is mainly caused by fractures. In 57 of 85 locations with leakage, the water originates from fractures. In the SKB geological mapping procedures, fractures have been subdivided into three subgroups according to the intensity of leakage, v, vv and vvv. Group “v” stands o for moist, group “vv” for dripping water and “vvv” stands for flowing water.

Water bearing fractures are concentrated to the set striking NW-SE and dipping sub-vertically. The “vv” and “vvv” fractures belong exclusively to this set perpendicular to the tunnel axis. Thus, the pattern in the TASQ is similar to that of the whole Äspö HRL where this set of NW-SE/sub-vertical fractures is associated with leakage. Although the “v” group spread more, it still shows some concentration to the same orientation.

In the geological mapping of the hole used for this data acquisition experiment, both fractures 08 and 14 (Figure 1-7) have “vvv” label and are therefore the more water bearing. They both belong to the set of sub-vertical fractures striking NW-SE (Table 1-2). These are the two fractures which displacements and inflow were monitored during the de-stressing of the pillar.

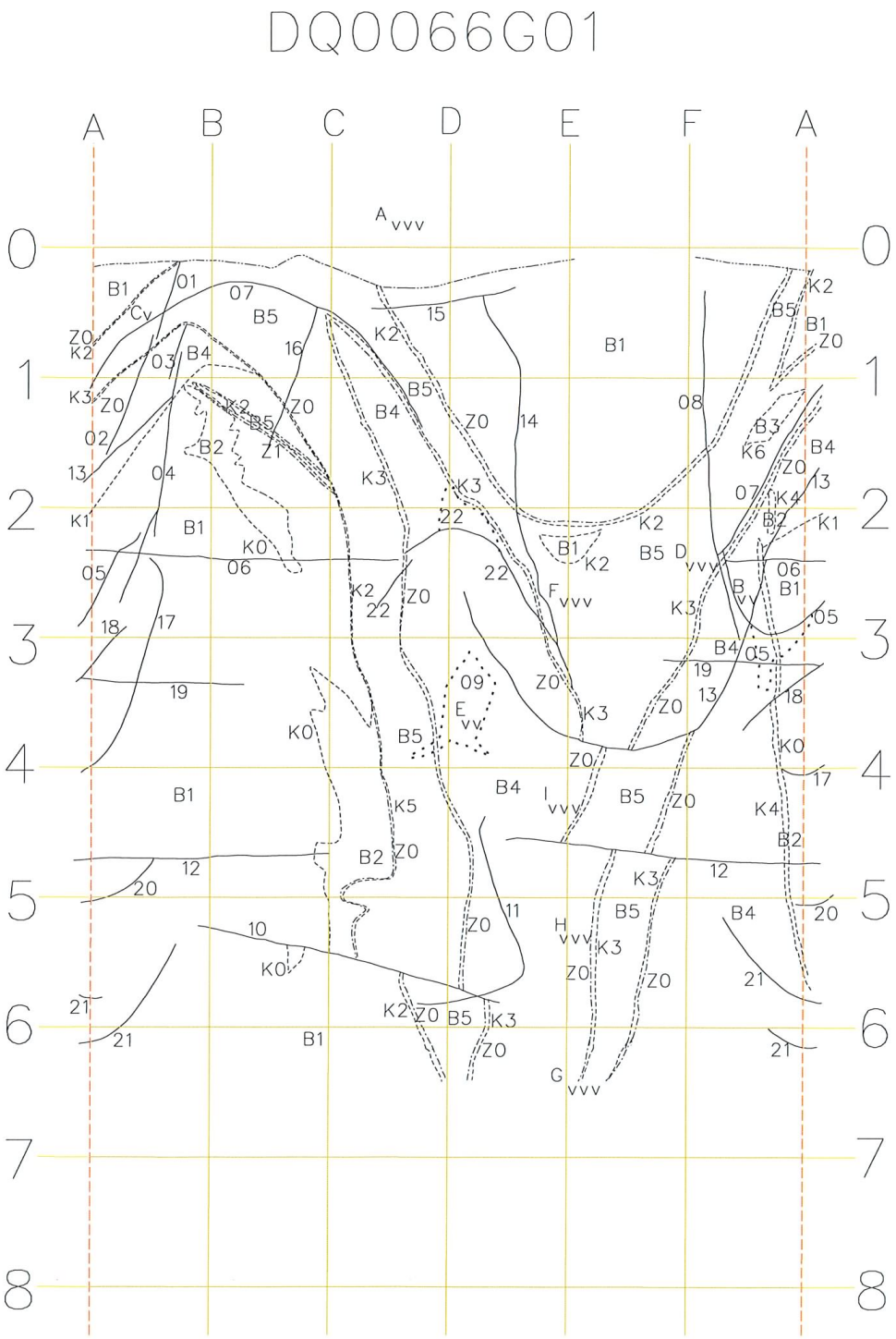

Figure 1-7. *Geological map of hole DQ006G01. Note the sub-vertical fractures 08 and 14.*

1.3 System geometry

The geometry of the tunnel TASQ was designed to concentrate and maximize the stresses in the centre of the tunnel floor (Figure 1-8).

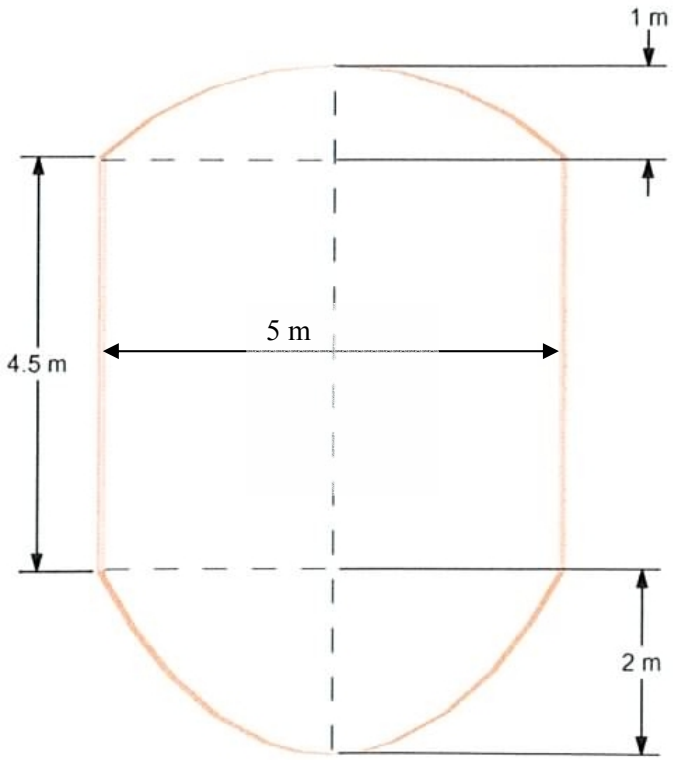

Figure 1-8. *Vertical section of tunnel TASQ /Staub et al, 2004/.*

A horizontal cross-section of the geometry of the experiment at tunnel floor level can be seen in Figure 1-2. The two deposition hole size excavations are located approximately along the axis of the tunnel and have a diameter of 1.8 m. The pillar between them has a width of 1m. Figure 1-9 shows the identification number of the holes as well as the identification number of the boreholes in the area used for several purposes (exploration, heating, acoustic emission, etc). The hole used for this data acquisition experiment (DQ0066G01) has a depth of 6.5 m while hole DQ0063G01 has a depth of 6.2 m.

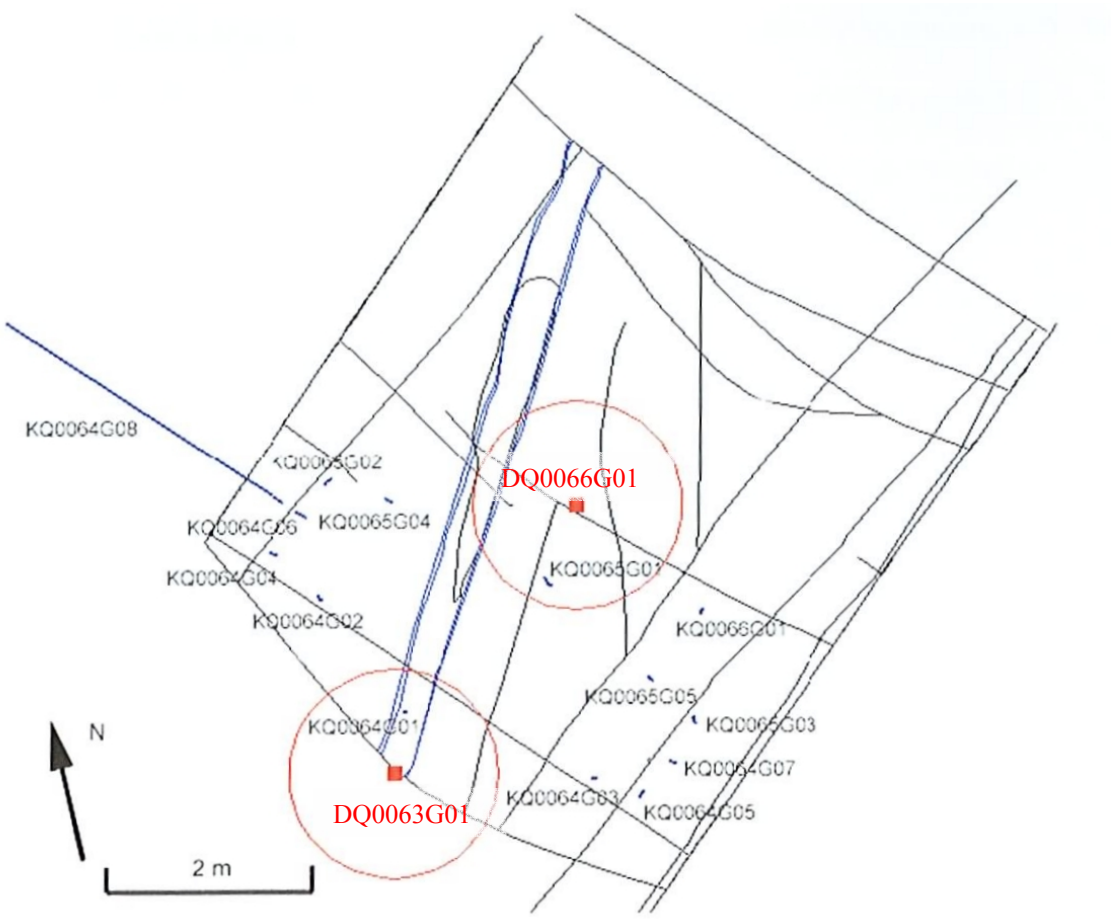

Figure 1-9. *Identification and location of the boreholes in the target area. The red cylinders represent the 1.8 diameter large holes /Staub et al, 2004/.*

1.4 Estimated stress evolution due to de-stressing of the pillar

A complete numerical study of the stress evolution during the APSE can be found in /Andersson, 2004a; Fredriksson et al, 2004; Rinne et al, 2004 and Wanne et al, 2004/.

The drilling of the de-stressing slot took place from the 25th to the 27th of October of 2004. The de-stressing slot shown in Figure 1-2, is composed of 27 boreholes of 64 mm diameter and 26 boreholes of 76 mm diameter (Figure 1-10). Table 1-8 shows the drilling time, depth and diameter of each borehole. Previous to the de-stressing slot, two small slots of 1 m depth were excavated nearby (additional slots in Figure 1-2) to avoid the cutter for the pillar to get jammed and to study the EDZ at the TASQ tunnel.

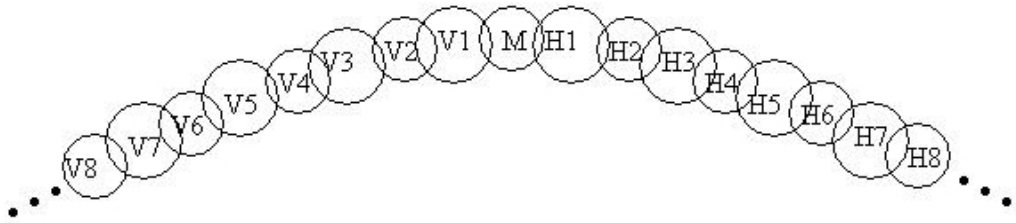

Figure 1-10. *Schematic plot showing the de-stressing slot borehole-drilling sequence according to Table 1-8.*

Table 1-8. De-stressing slot detailed borehole information.

Borehole ID.	Date	Drilling start time	Drilling stop time	Relative start time (sec)*	Relative stop time (sec)**	Depth (m)	Diameter (mm)
M	2004-10-25	07:34	07:48	471060	471900	7	64
H2	2004-10-25	07:56	08:13	472380	473400	7	64
V2	2004-10-25	08:20	08:29	473820	474360	7	64
H4	2004-10-25	08:35	08:46	474720	475380	7	64
V4	2004-10-25	09:35	09:47	478320	479040	7	64
H6	2004-10-25	10:00	10:11	479820	480480	7	64
V6	2004-10-25	10:17	10:30	480840	481620	7	64
H8	2004-10-25	10:34	10:46	481860	482580	7	64
V8	2004-10-25	10:50	11:02	482820	483540	7	64
H1	2004-10-25	11:14	11:27	484260	485040	7	76
H3	2004-10-25	11:28	11:33	485100	485400	7	76
V1	2004-10-25	11:35	11:39	485520	485760	7	76
V3	2004-10-25	12:30	12:38	488820	489300	6.3	76
H5	2004-10-25	12:40	12:47	489420	489840	6.5	76
H7	2004-10-25	12:57	13:03	490440	490800	6.6	76
V5	2004-10-25	13:31	13:39	492480	492960	6	76
V7	2004-10-25	14:29	14:35	495960	496320	5.8	76
H10	2004-10-25	14:43	14:45	496800	496920	7	64
V10	2004-10-25	15:01	15:14	497880	498660	7	64
V12	2004-10-26	08:15	08:27	559920	560640	7	64
V14	2004-10-26	08:33	08:45	561000	561720	7	64
H12	2004-10-26	08:51	09:02	562080	562740	7	64
H14	2004-10-26	09:39	09:52	564960	565740	7	64
V9	2004-10-26	10:03	10:09	566400	566760	4.5	76
V11	2004-10-26	10:10	10:24	566820	567660	5.5	76
V13	2004-10-26	10:36	10:41	568380	568680	5.8	76
H9	2004-10-26	10:51	11:00	569280	569820	5.7	76

H11	2004-10-26	11:03	11:07	570000	570240	5.7	76
H13	2004-10-26	11:24	11:31	571260	571680	7	76
V16	2004-10-26	13:37	13:49	579240	579970	7	64
V18	2004-10-26	13:58	14:10	580500	581220	7	64
H16	2004-10-26	14:18	14:29	581700	582360	7	64
H18	2004-10-26	14:37	14:49	582840	583560	7	64
H15	2004-10-26	14:54	15:02	583860	584340	6.1	76
H17	2004-10-26	15:06	15:11	584580	584880	6.4	76
V15	2004-10-26	15:16	15:23	585180	585600	5.4	76
V17	2004-10-26	15:26	15:33	585780	586200	6.4	76
H20	2004-10-27	07:48	08:08	644700	645900	7	64
H22	2004-10-27	08:10	08:22	646020	646740	7	64
H24	2004-10-27	08:28	08:40	647100	647820	7	64
H26	2004-10-27	08:46	08:57	648180	648840	6	64
H28	2004-10-27	09:03	09:15	649200	649920	7	64
H30	2004-10-27	10:15	10:27	653520	654240	7	64
H19	2004-10-27	10:35	10:43	654720	655200	6.2	76
H21	2004-10-27	10:45	10:48	655320	655500	6.4	76
H23	2004-10-27	10:54	11:03	655860	656400	5.2	76
H25	2004-10-27	11:05	11:10	656520	656820	7	76
H27	2004-10-27	11:12	11:17	656940	657240	6.2	76
H29	2004-10-27	11:18	11:25	657300	657720	6.3	76
V20	2004-10-27	13:45	13:59	666120	666960	7	64
V22	2004-10-27	14:05	14:20	667320	668220	7	64
V19	2004-10-27	14:30	14:37	668820	669240	6	76
V21	2004-10-27	14:40	14:54	669420	670260	6.2	76

* Approximate drilling start time in seconds for each borehole relative to the initiation of the monitoring.
** Approximate drilling stop time in seconds for each borehole relative to the initiation of the monitoring.

Figure 1-11 and Figure 1-12 show the estimated contours of Sigma_1 and Sigma_3 just before and after the de-stressing slot is drilled according to a continuum numerical simulation carried out by Christer Andersson from SKB /Andersson, 2004b/.

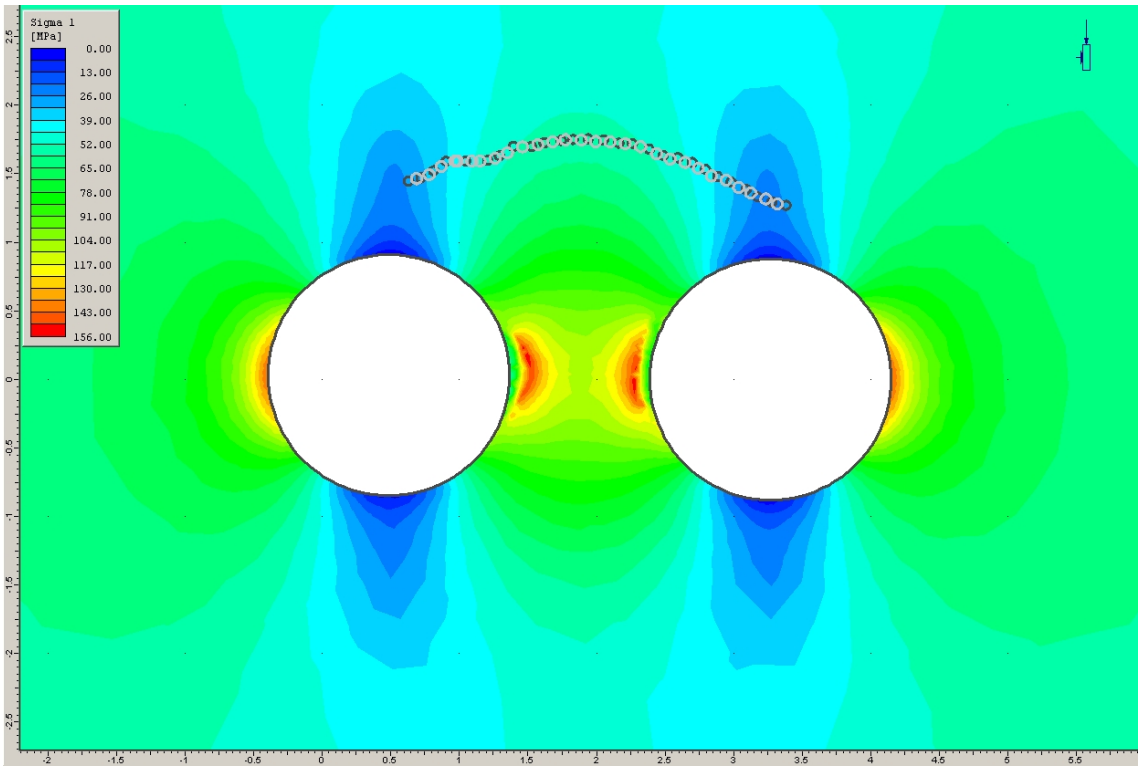

a)

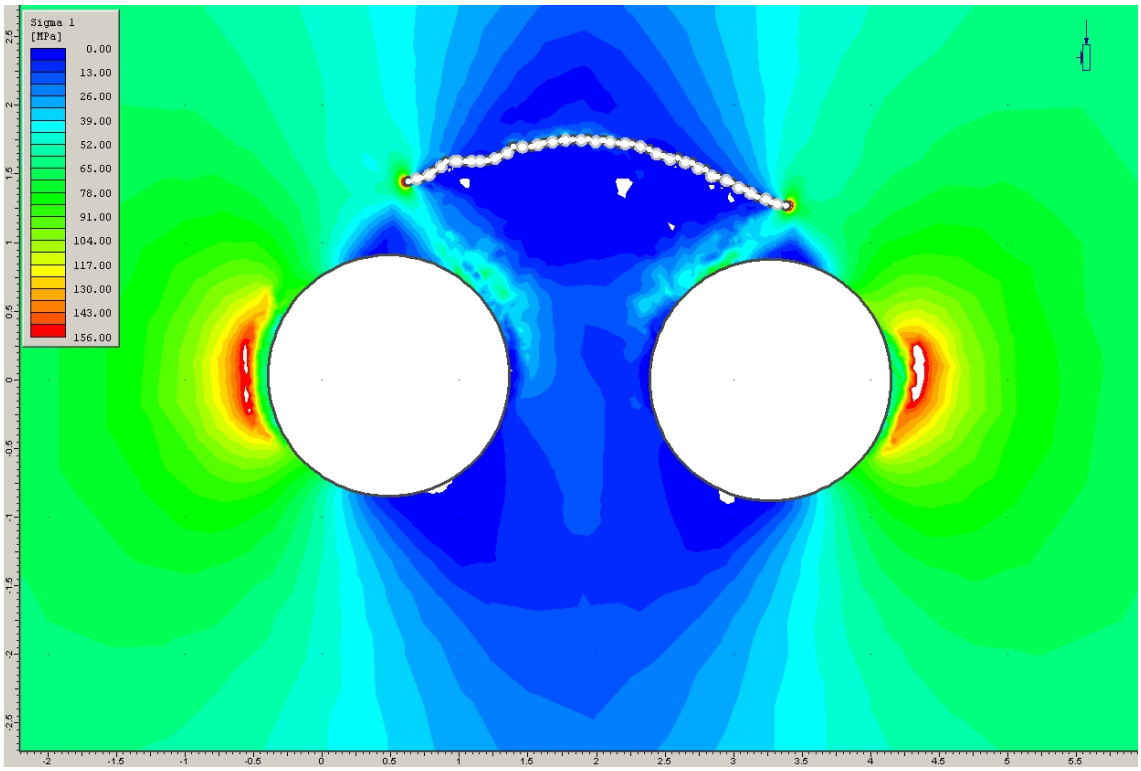

b)

Figure 1-11. *Estimated contours of the magnitude of Sigma_1 by continuum elastic numerical simulation: a) before, and b) after the drilling of the de-stressing slot /Andersson, 2004b/.*

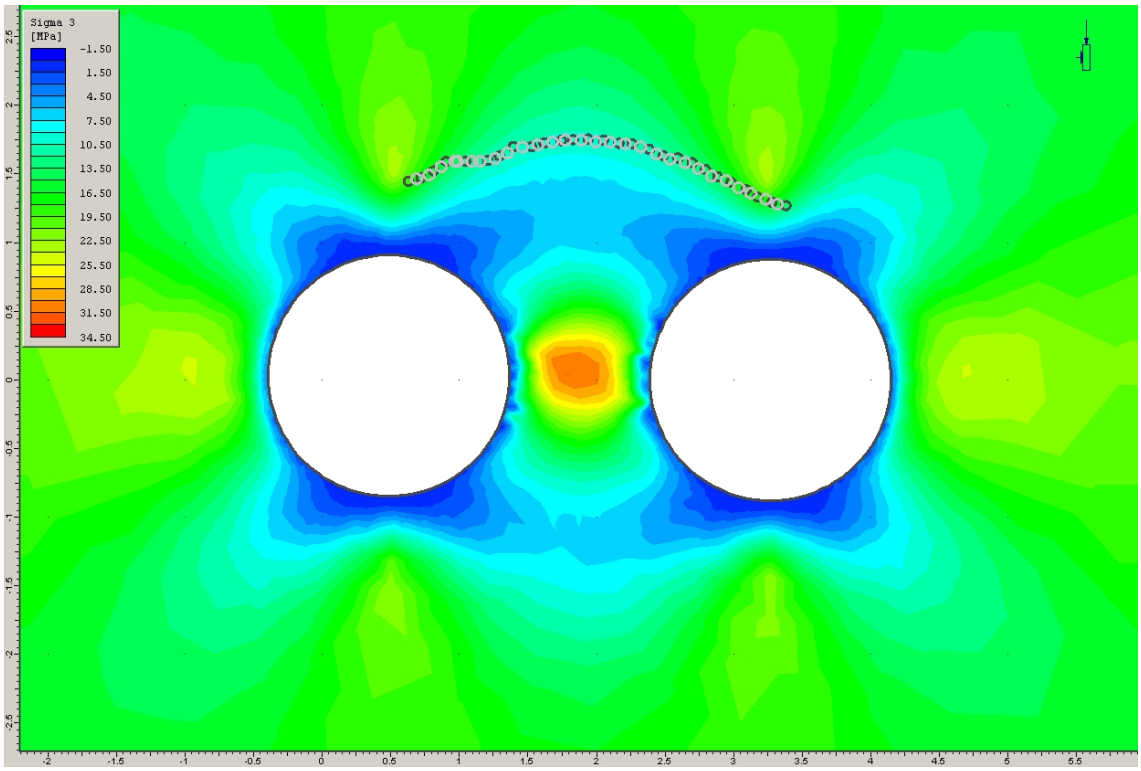

a)

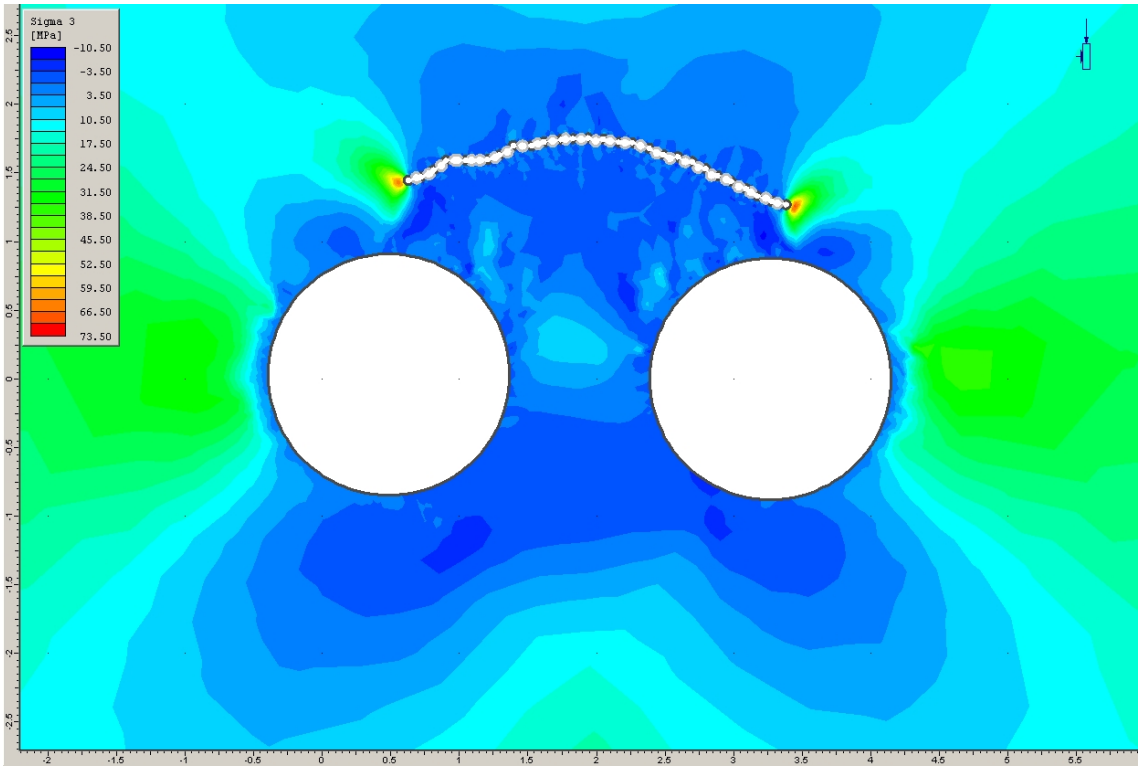

b)

Figure 1-12. *Estimated contours of the magnitude of Sigma_3 by continuum elastic numerical simulation: a) before, and b) after the drilling of the de-stressing slot /Andersson, 2004b/.*

1.5 Objectives

The data gathered in this project will help enhance the understanding about the hydro-mechanical behavior of fractured rocks, specially the coupled HM flow through single conductive fractures and inflow into excavations in hard rock.

The main objectives of this project are:

- Monitoring of the normal and shear displacements caused by the drilling of the de-stressing slot, along both conductive fractures responsible for the most part of the water inflow into the first hole drilled in the APSE project (Figure 1-2).
- Monitoring of the change in water inflow due to the drilling of the de-stressing slot, coming from each of the fractures selected.
- Monitoring of the change in total water inflow into the hole due to the drilling of the de-stressing slot.
- Monitoring of the water pressure at some boreholes in other locations in the Äspö HRL with the Hydro Monitoring System (HMS) to be able to asses the large scale influence of the drilling of the de-stressing slot.

2 Monitoring system

The drilling of the de-stressing slot in the APSE tunnel presented a unique opportunity to gather data about the influence of stress redistribution on the inflow into a deposition hole size excavation intersected by two very conductive sub-vertical fractures (Figure 1-2). Therefore, it was decided to install a monitoring system capable of continuously measuring the inflow coming from each one of the sub-vertical fractures as well as the total inflow into the hole. The monitoring system would also be capable of registering the normal and shear displacements in several locations along both fractures during the whole duration of the project.

The monitoring system was installed and controlled by Anders Eng and Rickard Karlzén at Äspö HRL. The whole monitoring system was connected to the SKB LAN so that the experiment could be followed in detail from surface at the Äspö HRL or anywhere with Internet access

The influence of the drilling of the de-stressing slot on other parts of the Äspö HRL would be studied by compiling and analyzing the pressure response measured in a number of selected boreholes in the level of the APSE tunnel via the Hydro Monitoring System (HMS).

2.1 Fracture displacements

For the displacement monitoring LVDT (Linear Variable Differential Transformer) type transducers were chosen. This type of sensor is accurate and robust in the harsh climate environment of the deposition hole. The measuring range of the LVDT used is 40 mm and the resolution, with the used configuration, is 10 μm.

A total number of ten LVDTs were installed. Table 2-1 shows the location and measurement type of each of them.

Table 2-1. LVDT location and type of measurement

LVDT ID.	Fracture ID.	Depth (m)	Measurement type
1	14	0.90	Horizontal shear displacement
2	14	1.20	Vertical shear displacement
3	14	1.20	Normal displacement
4	14	1.50	Horizontal shear displacement
5	08	0.90	Vertical shear displacement
6	08	0.95	Horizontal shear displacement
7	08	1.20	Normal displacement
8	08	1.80	Normal displacement
9	08	2.05	Horizontal shear displacement
10	08	2.60	Normal displacement

The following Figure 2-1 shows the LVDTs installed along the monitored fractures.

Figure 2-1. *LVDTs installed on the monitored fractures view from above).*

Figure 2.1 *(cont). LVDTs installed on the monitored fractures.*

2.2 Inflow

To be able to continuously register the inflow into the hole coming from each one of the sub-vertical fractures, a rubber channel was stack at 5 m depth. This channel collected the water from each of the two fractures and threw it into separate barrels (one for each fracture). One pressure meter measured the water head in each barrel and whenever the head value reached 70 cm a pump in the respective barrel extracted the water and threw it into the hole until the head in the barrel reached a value of 25 cm, in which case the pump stopped. This procedure was iteratively carried out for the whole duration of the experiment, allowing us to monitor the changes in inflow coming from each of the fractures.

A similar system was used for monitoring the total inflow into the hole. A pressure meter measured the head in the hole and whenever the value reached 20 cm a pump in the bottom of the hole extracted the water out of the excavation until the head reached a value of 10 cm, in which case it stopped.

The inflow coming from each of the fractures was monitored continuously without any problem for the whole project. However, the monitoring system for measuring the total inflow into the hole registered some wrong values due to momentary malfunction of the pressure meter and the pump in the bottom of the hole during some stages of the project.

The fracture inflow was monitored with an accuracy of ±5% and the total inflow had an accuracy of ±10%.

Figure 2-2 shows a picture of the water inflow monitoring system as described above.

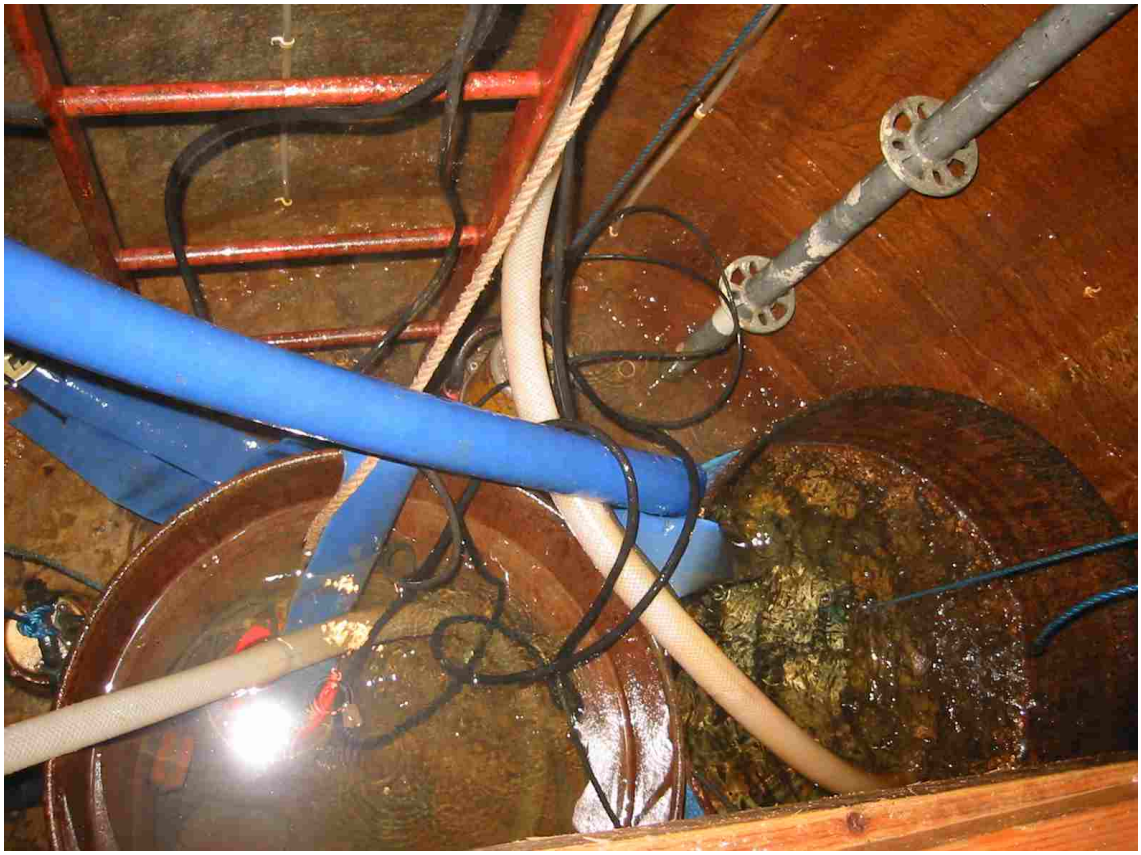

Figure 2-2. *Water inflow monitoring system.*

2.3 Hydro Monitoring System (HMS)

At Äspö HRL several boreholes are connected to a Hydro Monitoring System (HMS) that continually measures water pressure. Normally, this system records the pressure once every second hour and a detailed scanning starts when the measure pressure change exceeds 2 kPa.

To be able to judge the influence of the drilling of the de-stressing slot on other areas at the Äspö HRL, the pressure response was registered at a detailed scanning rate (once every 5 minutes) from a number of selected boreholes for the whole duration of the HM data acquisition experiment.

The boreholes expected to be influenced by the de-stressing slot were selected from published results /Fransson, 2003 and Staub et al, 2003/. The boreholes selected were: KA3385A, KA3510A, KI0025F, KA3386A01, KA3105A, KA3110A, KA2598A, KXTT4, KG0021A01, KG0048A01. Figure 2-3 shows their location at the Äspö HRL.

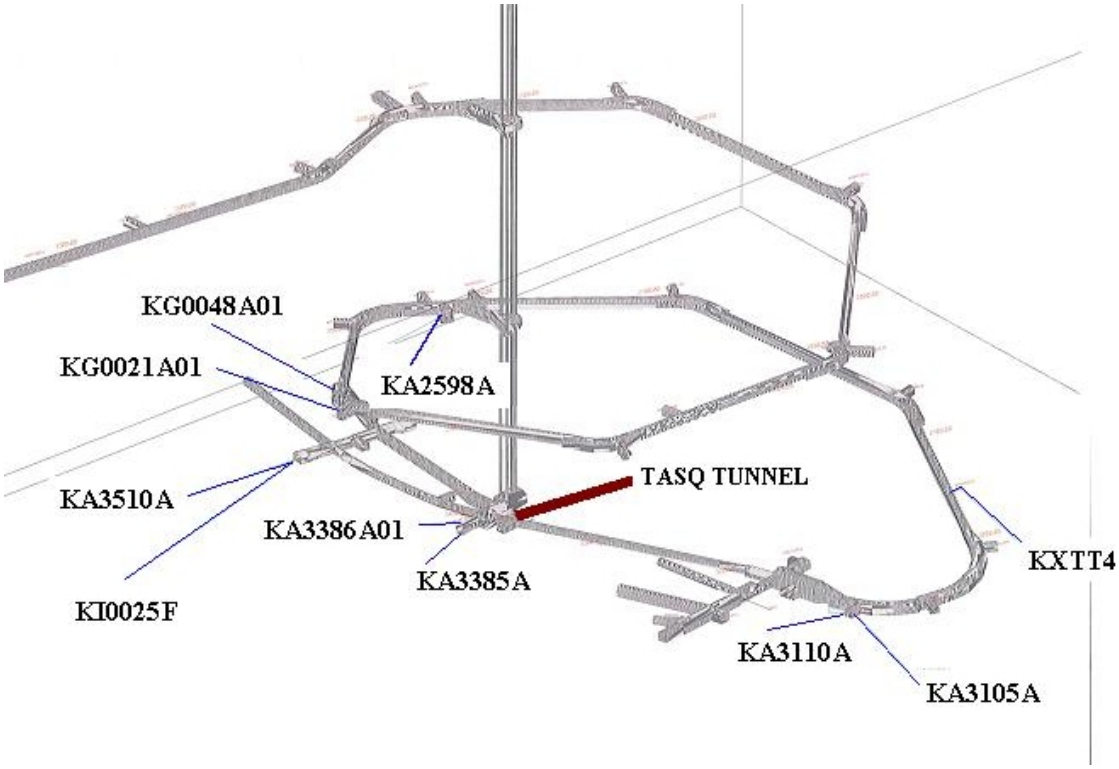

Figure 2-3. *Map of the Äspö HRL showing the location of the selected boreholes from the Hydro Monitoring System (in blue colour).*

3 Data collected

Once the TASQ tunnel was excavated, a number of vertical boreholes of 7 to 8 m depth were drilled on the floor of the APSE project area for different purposes (exploration, placement of heaters and acoustic emission devices, etc) before the two deposition-hole size excavations were drilled (Figure 1-9). Relevant data for the purpose of the HM acquisition experiment coming from some of these boreholes is summarized on the following paragraphs.

On the 5th of August 2003, the exploratory borehole KQ0065G01 was drilled. Beginning at about 1.90 m depth an initial inflow of 40 l/min was measured. On the 16th of September the inflow had reached a steady state value of 1.27 l/min.

On the 12th of August 2003, the acoustic emission borehole KQ0065G05 was drilled. From a depth of 5 m onwards an initial inflow of 30 l/min was measured. On the 16th of September the inflow had reached a steady state of 6.21 l/min. According to the core from this borehole fracture 08 was intersected at about 5 m depth.

On the 13th of August 2003, the heater borehole KQ0065G03 was excavated. It was dry until reaching a depth of 6.15 m, where it intersects fracture 08 according to the drill core. The initial inflow registered was 25 l/min. The 16th of September the inflow had reached a steady state of 4.19 l/min.

On the 29th of August 2003, the borehole KQ0065G04 was drilled and it was found to be completely dry.

Finally, on the 2nd of December 2003, when the first of the two holes was excavated (DQ0066G01) the approximated total inflow measured was 30 l/min.

3.1 Fracture displacements

The figures in this section show the normal and shear displacements along fractures 08 and 14 (Figure 1-2) due to the drilling of the de-stressing slot in the APSE site.

In Figure 3-1 we can see the normal and shear displacements in fracture 08 at different depth along the fracture. According to the graph, the normal displacement (fracture opening in this case) is more pronounced at 1.8 m and 2.6 m depth than at 1.2 m depth. The maximum opening measured (at 2.6 m depth) is 0.6 mm approximately. The opening of fracture 08 was expected according to the expected decrease in normal stress acting on the fracture plane.

Regarding shear displacement, it is worth to point out the low value of shear in the vertical direction compared to the horizontal direction. The maximum shear measured in horizontal direction (at 0.95 m depth) is approximately 0.9 mm (Figure 3-1).

The displacements along fracture 14 are shown in Figure 3-2. The fracture at 1.2 m depth is closing slightly (up to 0.07 mm closure) which is reasonable according to the expected increase in normal stress acting on the fracture plane as the drilling of the de-stressing slot is carried out. However, it is believed that some other parts of fracture 14

could open slightly due to the dilation caused by shear displacement. Shear displacement could also be the cause of the reactivation of flow channels. Shear dilation and reactivation of flow channels due to shear movement could be the explanation of the observed increase in inflow caused by the drilling of the slot. As in fracture 08, the shear displacement is larger in the horizontal direction than on the vertical direction. The maximum shear displacement registered is approximately 0.29 mm.

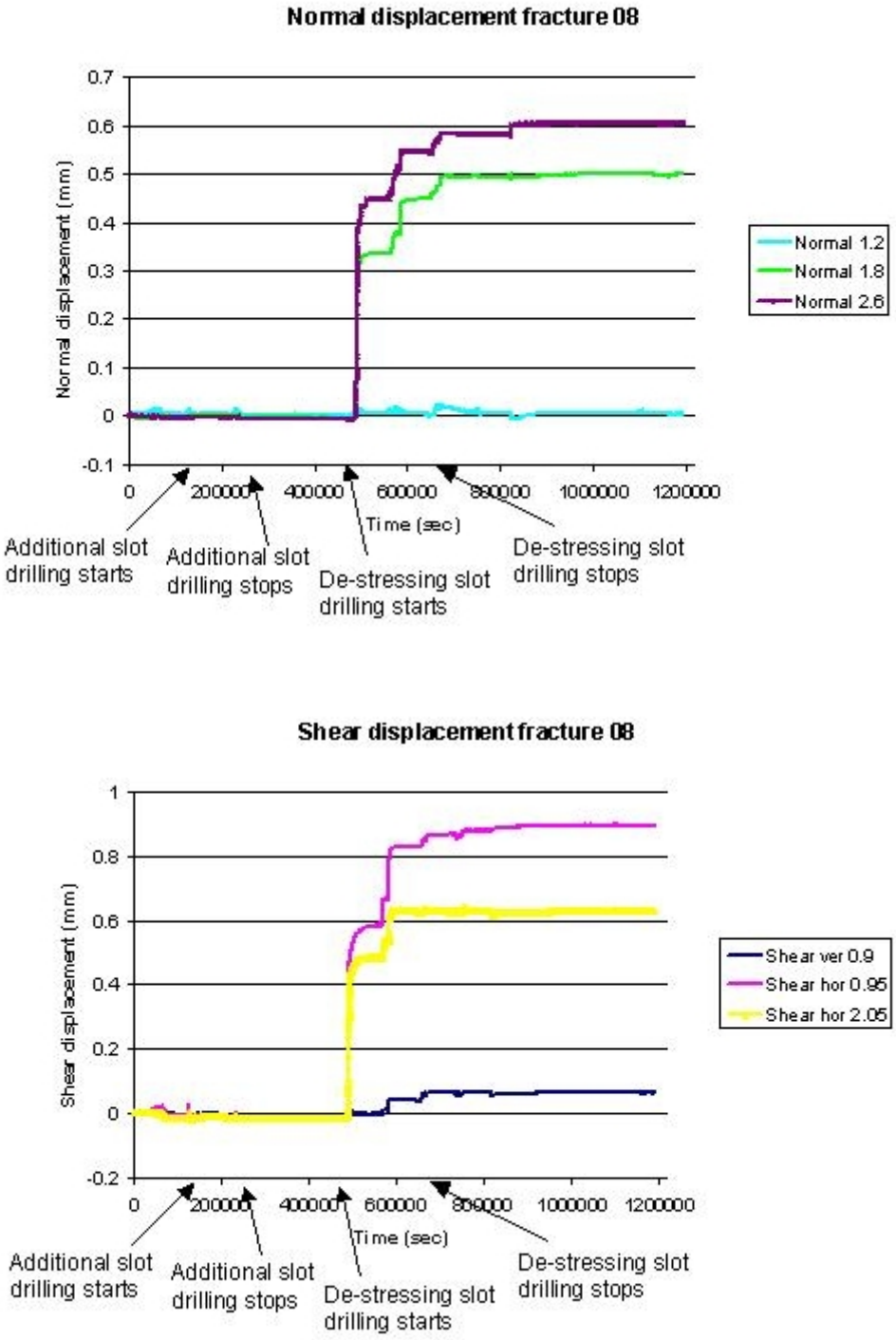

Figure 3-1. *Normal and shear displacement measured on fracture 08. The numbers in the legends indicate the depth in the measurement location along the fracture.*

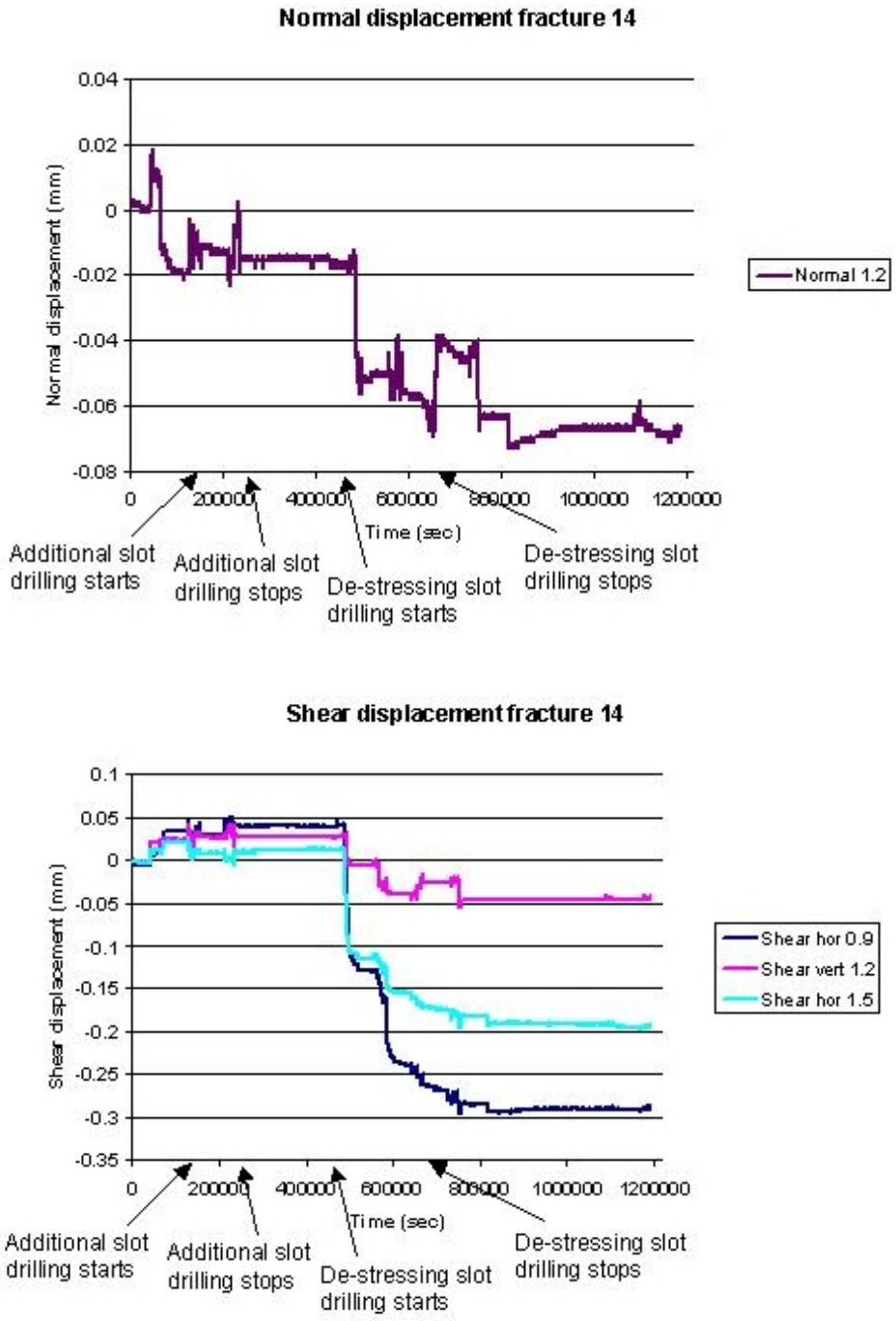

Figure 3-2. *Normal and shear displacement measured on fracture 14. The numbers in the legends indicate the depth in the measurement location along the fracture.*

Figure 3-3 and Figure 3-4 present a close up of the previous Figure 3-1 and Figure 3-2 respectively. They include the drilling time of the most relevant boreholes. As can be observed, when borehole V3 is drilled, both normal and shear movements begin to occur in both fractures.

After the displacement has been triggered after borehole V3 is drilled, other specific boreholes are the responsible of triggering further displacements in the fractures at different depths like borehole V17, V12, H12, V9, H20, H23, etc.

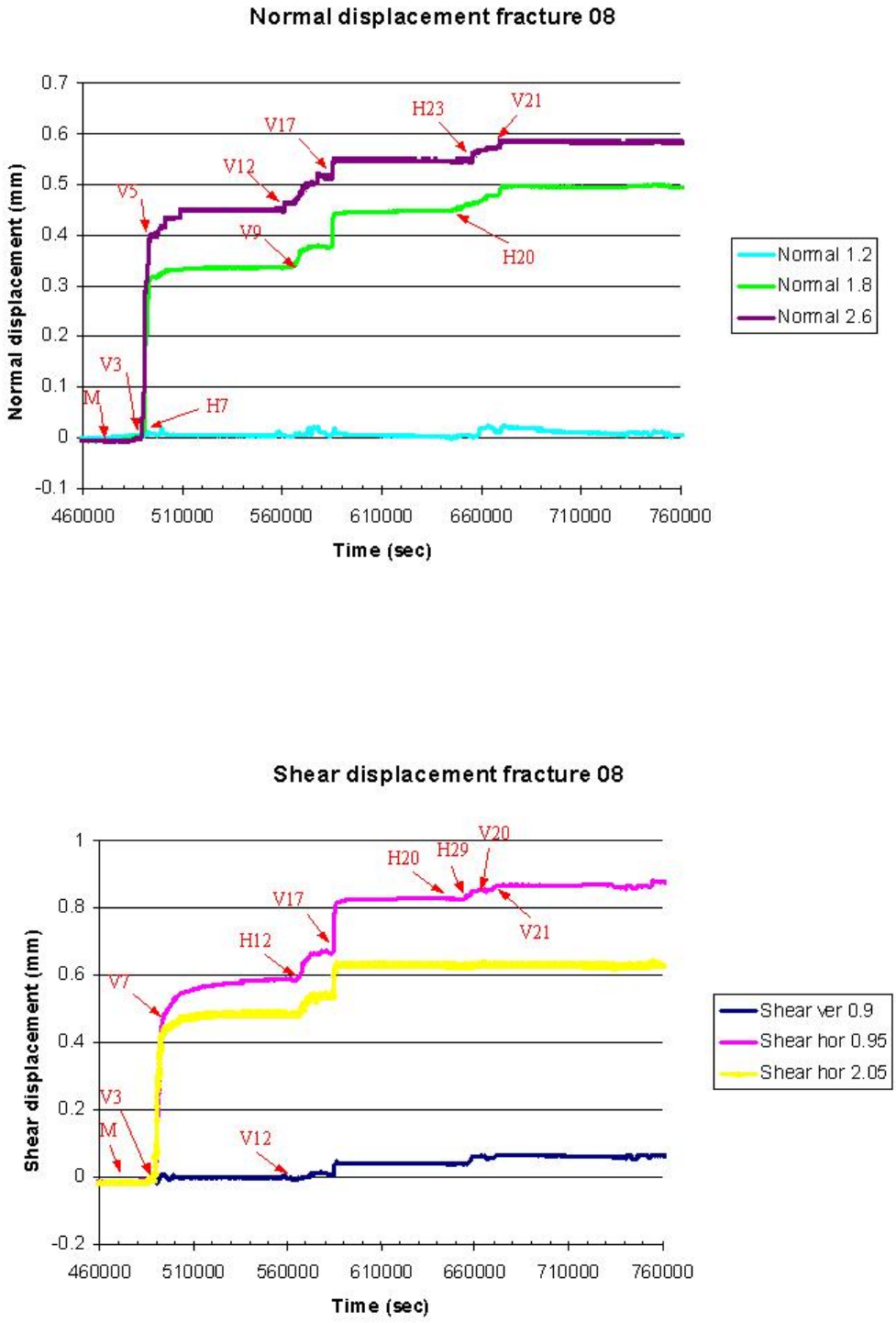

Figure 3-3. *Zoom in of the normal and shear displacement measured on fracture 08 with the drilling time of the most relevant boreholes indicated. The numbers in the legends indicate the depth in the measurement location along the fracture.*

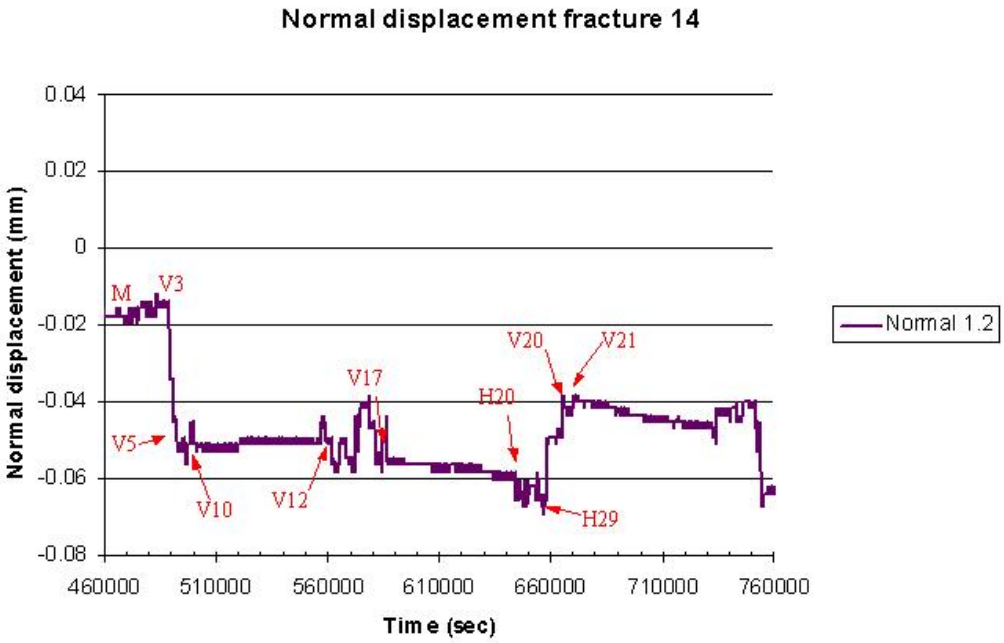

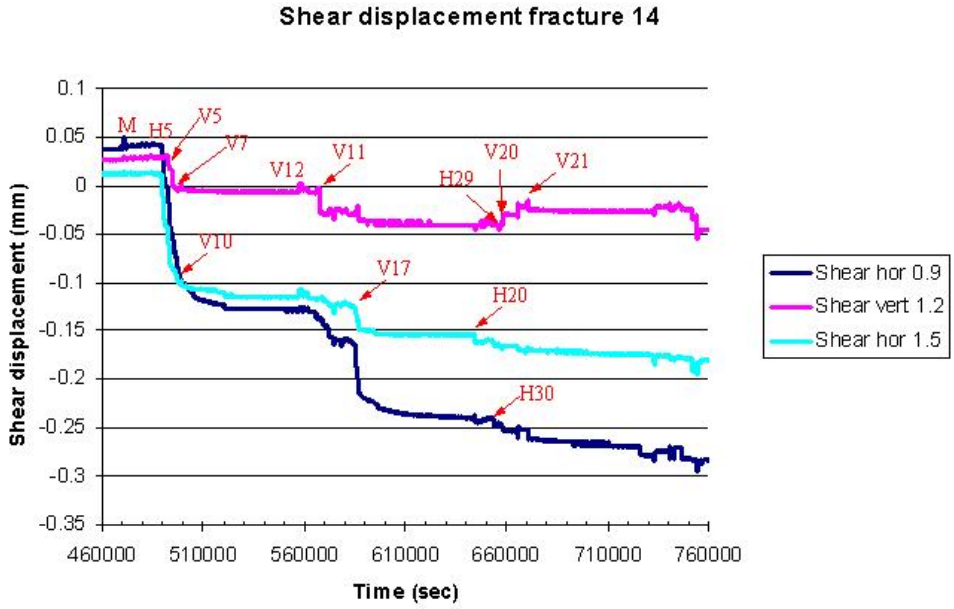

Figure 3-4. *Zoom in of the normal and shear displacement measured on fracture 14 with the drilling time of the most relevant boreholes indicated. The numbers in the legends indicate the depth in the measurement location along the fracture.*

3.2 Inflow

The change in water inflow registered during the drilling of the de-stressing slot is shown in Figure 3-5 and Figure 3-6.

As can be seen in Figure 3-5a, the drilling of the additional slot decreased the inflow coming from fracture 14. However, the inflow coming from fracture 08 experiences only reversible changes during this time. This agrees well with the displacement data in Figure 3-1 and Figure 3-2 where the influence of the additional slot is more noticeable in fracture 14 than in fracture 08.

In both fractures, the inflow after the de-stressing slot has been drilled is double than that before the drilling (the inflow coming from fracture 08 increases from 2.4 l/min to 4 l/min and the inflow from fracture 14 increases from 6.1 l/min to 18 l/min). As shown in Figure 3-5b, the most dramatic change in inflow comes when boreholes V3 to V7 are drilled (Table 1-8), which once again, agrees well with the fracture displacement data presented in the previous section.

As can be seen in Figure 3-5a, there is a sudden increase in the inflow measured in fracture 08 after the drilling of the de-stressing slot has finished. This is due to the fact that borehole KQ0065G03 (Figure 1-9) which intersects fracture 08 at about 6.15 m depth, was open during the whole duration of the drilling of the de-stressing slot, and it was draining the water from fracture 08 before reaching the hole. Afterwards, it was closed and the inflow coming to the hole from fracture 08 increased exactly the same amount as what was being drained from the borehole (4.19 l/min).

In Figure 3-6 we can see the water inflow coming from both fractures together, the inflow coming from everywhere else in the hole, and the total inflow into the hole, for the whole duration of the experiment. The total inflow into the hole could not be measured at all times due to some difficulties with the pump and the pressure meter in the hole.

It is important to notice in Figure 3-6 that the sum of the inflow coming from the two monitored fractures before the drilling of the de-stressing slot is of the same order as the inflow coming from elsewhere in the hole. It can be assumed that the increase in fracture inflow due to the closure of borehole KQ0065G03 after the drilling of the de-stressing slot would have the same effect if it had been closed before the drilling of the slot. In this case the inflow coming from the fractures before the drilling of the slot would have been approximately 60 % of the total inflow.

The inflow coming from elsewhere, due to matrix flow and small cracks (“dep. hole, no fractures” in the legend in Figure 3-6), experiences mainly reversible changes during the drilling of the de-stressing slot, and after the drilling it comes again approximately to its initial value.

On the other hand, the inflow coming from both fractures increases irreversibly with the drilling of the de-stressing slot and becomes at the end two thirds of the total inflow into the hole, while initially it was only half of the total inflow Figure 3-6. After the closure of the borehole KQ0065G03, the inflow coming from the fractures monitored becomes 72 % of the total inflow.

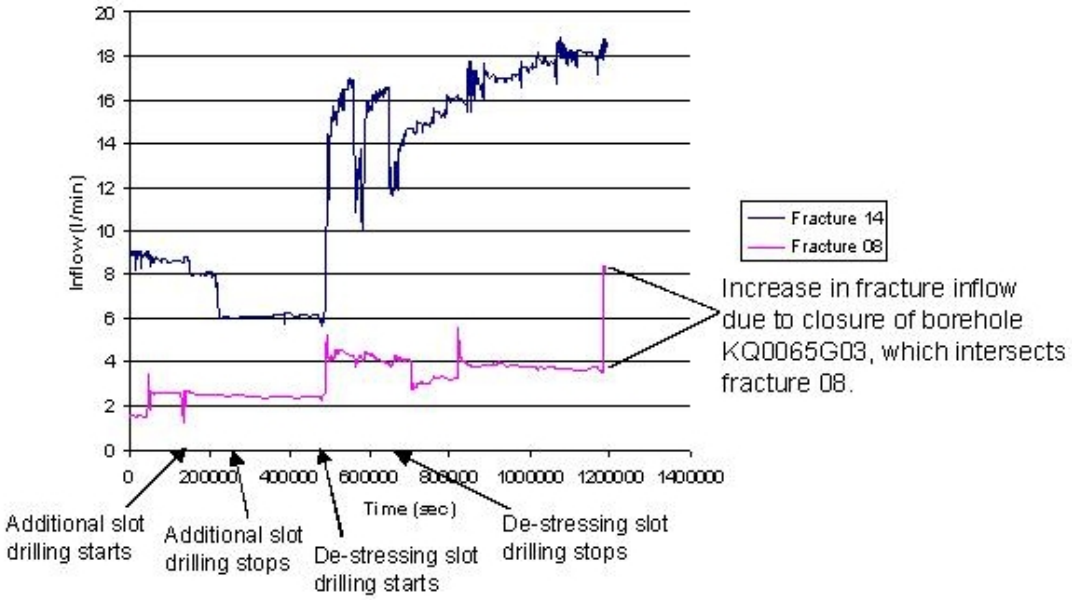

a) *all the monitored time*

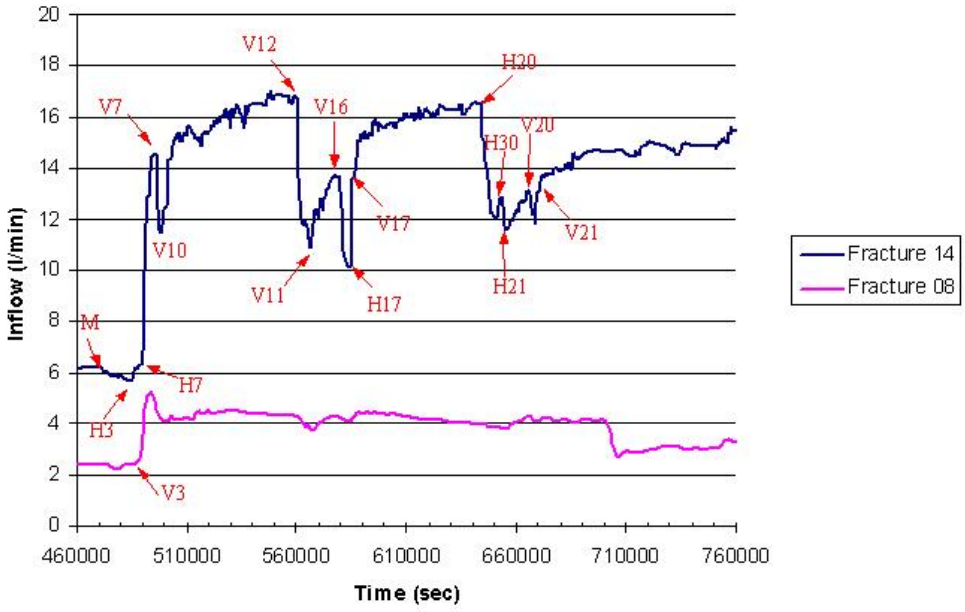

b) *Zoom in with the drilling time of the most relevant boreholes indicated*

Figure 3-5. *Water inflow into hole DQ0066G01 coming from fractures 08 and 14 for: a) all the monitored time, and b) the duration of the drilling of the de-stressing slot.*

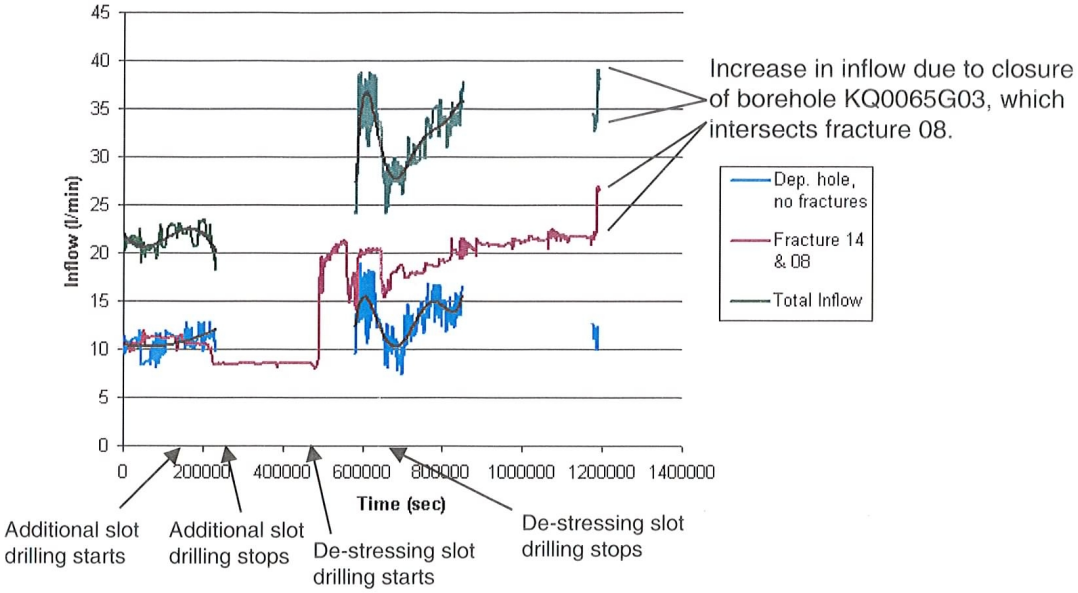

Figure 3-6. *Water inflow into hole DQ0066G01 from the fractures monitored (08 & 14), from elsewhere in the hole, and total water inflow for the total duration of the monitoring time.*

3.3 Large scale hydraulic influence of the de-stressing slot (HMS)

The influence of the drilling of the de-stressing slot and the subsequent local stress redistribution on the surroundings of the APSE volume at the Äspö HRL was investigated by compiling water pressure responses in a number of selected boreholes using the hydro monitoring system.

Strong responses were registered in boreholes KA3385A, KA3386A01 and KA2598A. A weak response was registered in borehole KI0025F. The rest of the boreholes selected had no noticeable response to the drilling of the de-stressing slot (Figure 3-7).

The water pressure response registered in boreholes KA2598A and KA3386A01 can be seen in Figure 3-8 and Figure 3-9 respectively. The figures from the rest of the boreholes selected can be found in Appendix A.

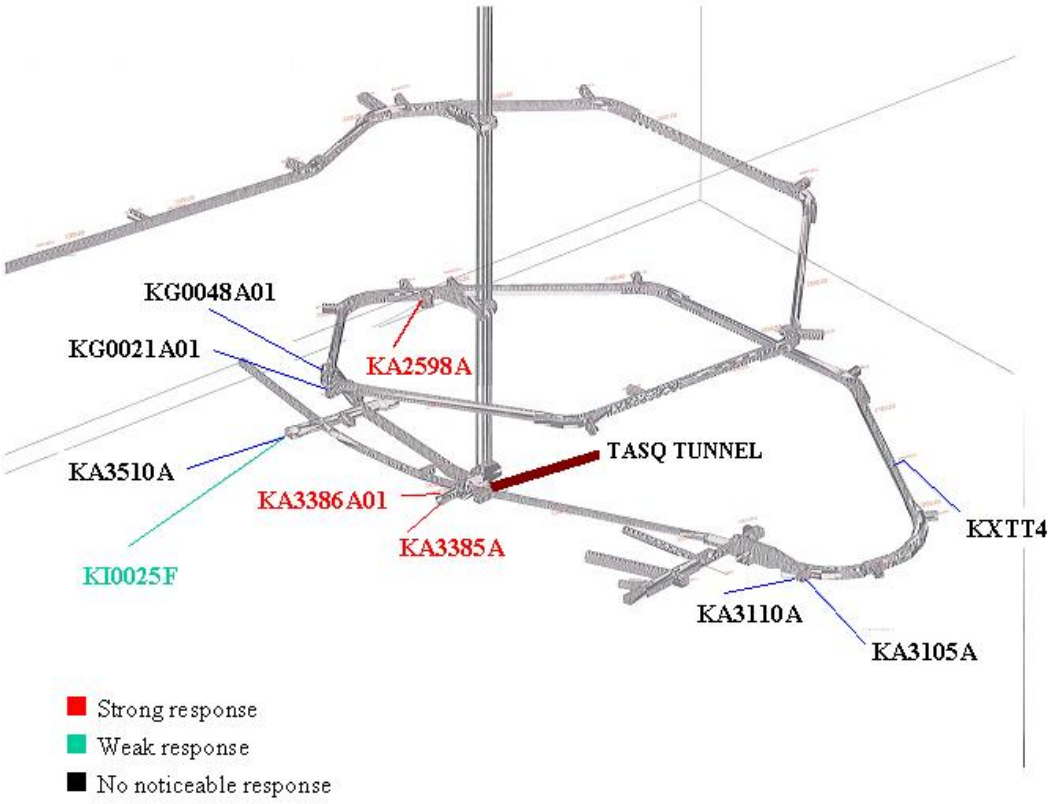

Figure 3-7. *Map of the Äspö HRL showing the location of the selected boreholes from the Hydro Monitoring System and the intensity of the registered water pressure response due to the drilling of the de-stressing slot at the APSE site (TASQ tunnel).*

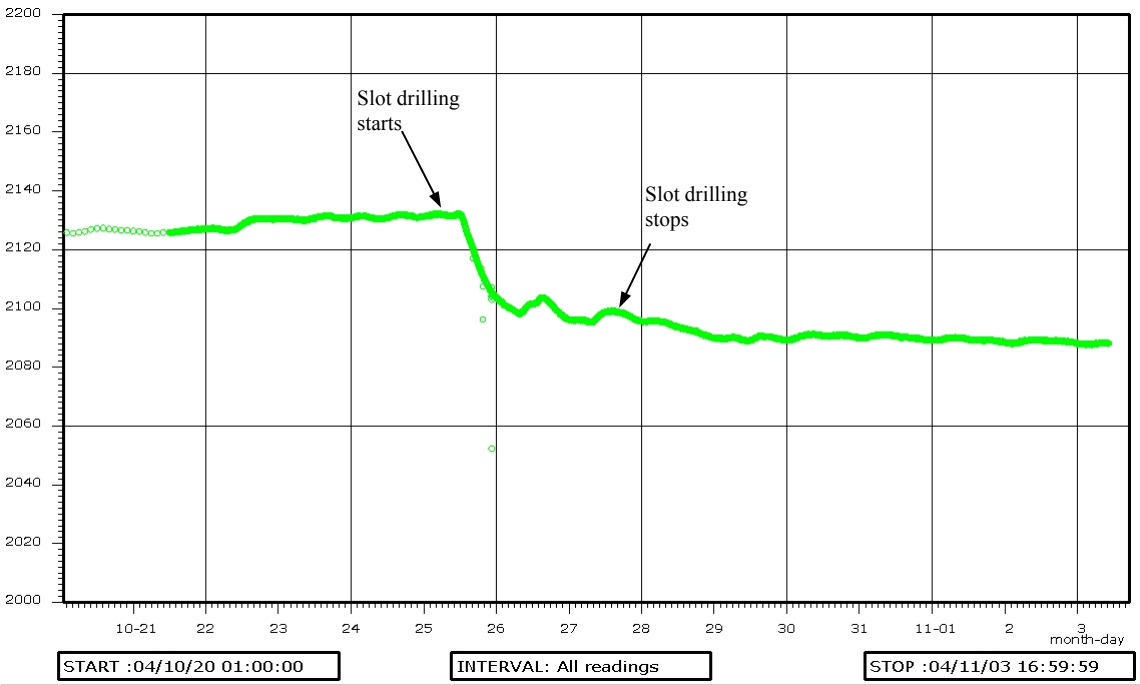

Figure 3-8. *Registered water pressure response (kPa) at borehole KA2598A during the period of the drilling of the de-stressing slot at the APSE site.*

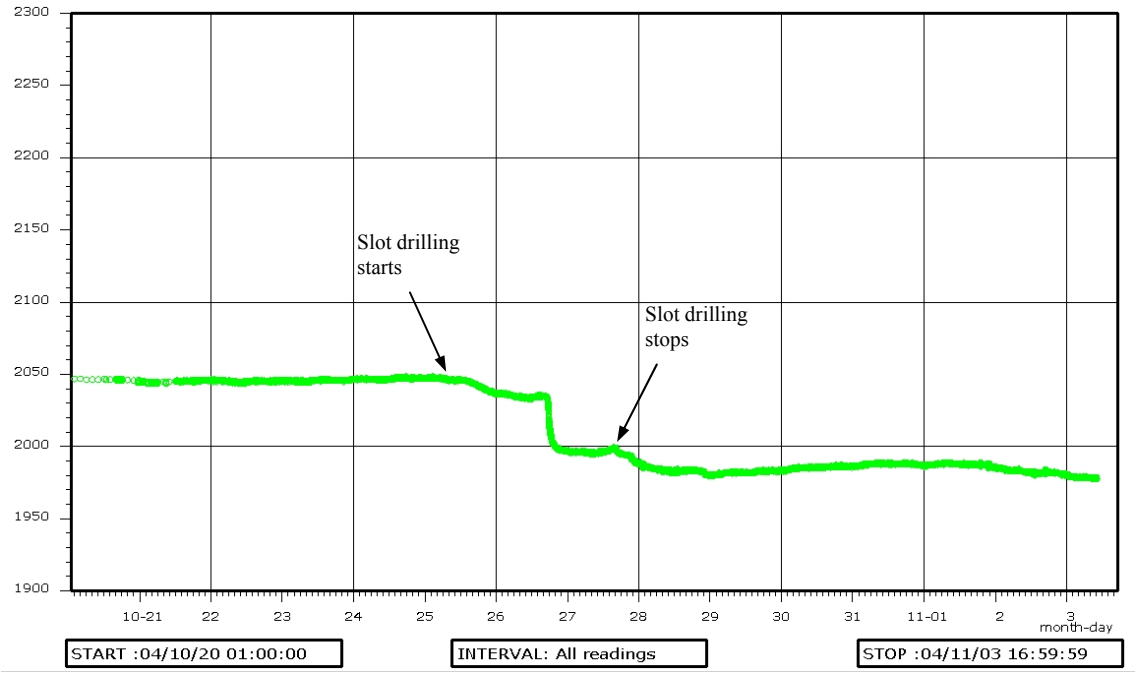

Figure 3-9. *Registered water pressure response (kPa) at borehole KA3386A01 during the period of the drilling of the de-stressing slot at the APSE site.*

4 Conclusions

A large-scale field test has been conducted at the Äspö HRL in which fracture displacements, fracture inflow, and total inflow have been monitored in the hole DQ0066G01 during the drilling of the de-stressing slot at the APSE site.

The fractures monitored (fractures 08 and 14) belong to the set striking NW-SE and dipping sub-vertically and they both are highly conductive and intersect the deposition hole size vertical borehole DQ0066G01 (Figure 1-2).

The maximum normal displacement (opening) in fracture 08 is 0.6 mm (Figure 3-1), which agrees well with the fact that the normal stress acting on this fracture is expected to decrease with the drilling of the de-stressing slot. On the other hand, the normal stress acting on fracture 14 is expected to increase with the drilling of the slot and this can explain the negative normal displacement registered (-0.07 mm), which indicates closure (Figure 3-2). However, due to the fact that fractures will often displace in a compressional situation, it is possible that some other parts of fracture 14 could open due to the dilation caused by shear displacement. This shear displacement could also be the cause of the reactivation of flow channels. Therefore, shear dilation and reactivation of flow channels due to shear movement could be the cause of the observed increase in inflow caused by the drilling of the slot (Figure 3-5).

The shear displacement registered is larger for both fractures in the horizontal direction than in the vertical direction (neglectable compared to the horizontal shear). The maximum shear displacement registered in fracture 08 is approximately 0.9 mm and in fracture 14 is 0.29 mm.

According to the drilling sequence (Table 1-8 and Figure 1-10) the largest displacements are initiated when borehole V3 is drilled (Figure 3-3 and Figure 3-4).

In both fractures, the inflow after the de-stressing slot has been drilled is double than that before the drilling (the inflow coming from fracture 08 increases from 2.4 l/min to 4 l/min and the inflow from fracture 14 increases from 6.1 l/min to 18 l/min) (Figure 3-5a). On the other hand, the inflow coming from elsewhere in the hole but the two fractures (due to matrix flow and small cracks), experiences mostly reversible changes and is approximately the same at the end of the drilling. As a consequence, while the inflow coming from both fractures before the drilling of the slot accounted for 60% of the total inflow, after the drilling it accounted for approximately 72% of the total inflow (*Figure 3-6*).

The most dramatic increase in inflow coming from both fractures occurs when boreholes V3 to V7 are drilled (Figure 3-5b).

During the drilling of the slot several boreholes in the HMS system were selected to assess the influence of the de-stressing on other locations at the Äspö HRL. Strong responses were found in boreholes KA3385A, KA3386A01 and KA2598A. A weak response was also registered in borehole KI0025F. In the rest of the boreholes selected there was no noticeable response (Figure 3-7).

The data gathered in this project can help enhance the knowledge about coupled hydro-mechanical processes in fractured hard rock and it could be used as input for an analytical and numerical study based on this field experiment. Additional input regarding the following aspects would improve the quality of such a study:

- The total extension of both fractures monitored is not known. As the fracture shear displacement is correlated with the fracture length /La Pointe et al, 1997; Hakami and Olofsson, 2002; Hökmark, 2003 and Mas Ivars, 2004/, any assumption about the length of the fractures could affect the mechanical and hydraulic response of the system.

- The pore water pressure in the area of the experiment has not been monitored and therefore it would need to be approximated from data from boreholes in the vicinity.

- Future studies would benefit from input regarding the mechanical properties of both fractures monitored. Although fractures from the same set at Äspö HRL have been tested previously in the laboratory, the acquisition of specific information about the mechanical behavior of these two fractures would help improve future analyses.

- When fractures are under moderate to high normal stresses, the flow can deviate from the cubic law due to tortuosity /Cook, 1992 and Hopkins, 2000/. The tortuosity is an increasing function of the contact area in the fracture and, therefore, it will increase as the stress increases /Zimmerman et al, 1990/. A future analytical and numerical study of the data presented in this report would benefit from a proper characterization of the hydro-mechanical behavior of the fractures monitored. This could be achieved by characterization of the fracture surfaces and coupled shear-flow laboratory tests of samples from those two fractures. This would help improve and adjust already existing coupled stress-flow fracture constitutive models so this type of fractures can be better represented in future studies.

References

Andersson J C, 2004a. Äspö Pillar Stability Experiment. Summary of preparatory work and predictive modelling. *SKB*, *R-03-02. Svensk Kärnbränslehantering.*

Andersson J C, 2004b. Personal communication.

Cook N G W, 1992. Natural joints in rock: mechanical, hydraulic, and seismic behavior and properties under normal stress. Int. J. Rock Mech. Min. Sci. Geomech. Abstr. No. 29 (3), pp. 198-223.

Fransson Å, 2003. Äspö Hard Rock Laboratory. Äspö Pillar Stability Experiment. Core boreholes KF0066A01, KF0069A01, KA3386A01 and KA3376B01: Hydrogeological characterization and pressure responses during drilling and testing. *SKB, IPR-03-06. Svensk Kärnbränslehantering.*

Fredriksson A, Staub I and Outers N, 2004. Äspö Pillar Stability Experiment. Final 2D coupled thermo-mechanical modelling. *SKB*, *R-04-02. Svensk Kärnbränslehantering.*

Hakami E and Olofsson S-O, 2002. Numerical modeling of fracture displacements due to thermal load from a KBS-3 repository, SKB, *TR-02-08. Svensk Kärnbränslehantering.*

Hökmark H, 2003. Canister Positioning. Influence of fracture system on deposition hole stability, SKB, *R-03-19. Svensk Kärnbränslehantering.*

Hopkins D L, 2000. The implications of joint deformation in analyzing the properties and behavior of fractured rock masses, underground excavations, and faults. Int. J. Rock Mech. Min. Sci. No. 37, pp. 175-202.

Jarsjö J, Destouni G and Gale J, 2001. Groundwater degassing and two-phase flow in fractured rock: Summary of results and conclusions achieved during the period 1994-2000. *SKB, TR-01-13. Svensk Kärnbränslehantering.*

La Pointe P, Wallmann P, Thomas A and Follin S, 1997. A methodology to estimate earthquake effects on fractures intersecting canister holes, SKB, *TR-97-07, Svensk Kärnbränslehantering.*

Magnor B, 2004. Äspö Hard Rock Laboratory. Äspö Pillar Stability Experiment. Geological mapping of tunnel TASQ. *SKB, IPR-04-03. Svensk Kärnbränslehantering.*

Mas Ivars D, 2004. Inflow into excavations – a coupled hydro-mechanical three-dimensional numerical study. *Licentiate Thesi*s. *KTH, Stockholm, Sweden.*

Olsson O, 1992. Site characterization and validation – Final report. Stripa Project. *SKB, TR-92-22. Svensk Kärnbränslehantering.*

Rhén I and Forsmark T, 2001. Prototype repository. Hydrogeology – Summary report of investigations before the operations phase. Äspö Hard Rock Laboratory. *SKB, IPR-01-65. Svensk Kärnbränslehantering.*

Rinne M, Shen B and Lee H-S, 2004. Äspö Pillar Stability Experiment. Modelling of fracture development of APSE by FRACOD. *SKB*, *R-04-04. Svensk Kärnbränslehantering.*

Staub I, Andersson J C and Magnor B, 2004. Äspö Pillar Stability Experiment. Geology and mechanical properties of the rock in TASQ. *SKB*, *R-04-01. Svensk Kärnbränslehantering.*

Staub I, Janson T and Fredriksson A, 2003. Äspö Hard Rock Laboratory. Äspö Pillar Stability Experiment. Geology and properties of the rock mass around the experiment volume. *SKB, IPR-03-02. Svensk Kärnbränslehantering.*

Wanne T, Johansson E and Potyondy D, 2004. Äspö Pillar Stability Experiment. Final coupled 3d thermo-mechanical modeling. Preliminary particle-mechanical modeling. *SKB*, *R-04-03. Svensk Kärnbränslehantering.*

Zimmerman R W, Chen D W, Long J C S and Cook N G W, 1990. Hydromechanical coupling between stress, stiffness, and hydraulic conductivity of rock joints and fractures. In: Barton N. Stephansson. O. editors. Proc. Int. Symp. On Rock Joints. Rotterdam: Balkema, 1990. pp. 571-577.

Appendix A: water pressure response in selected HMS boreholes

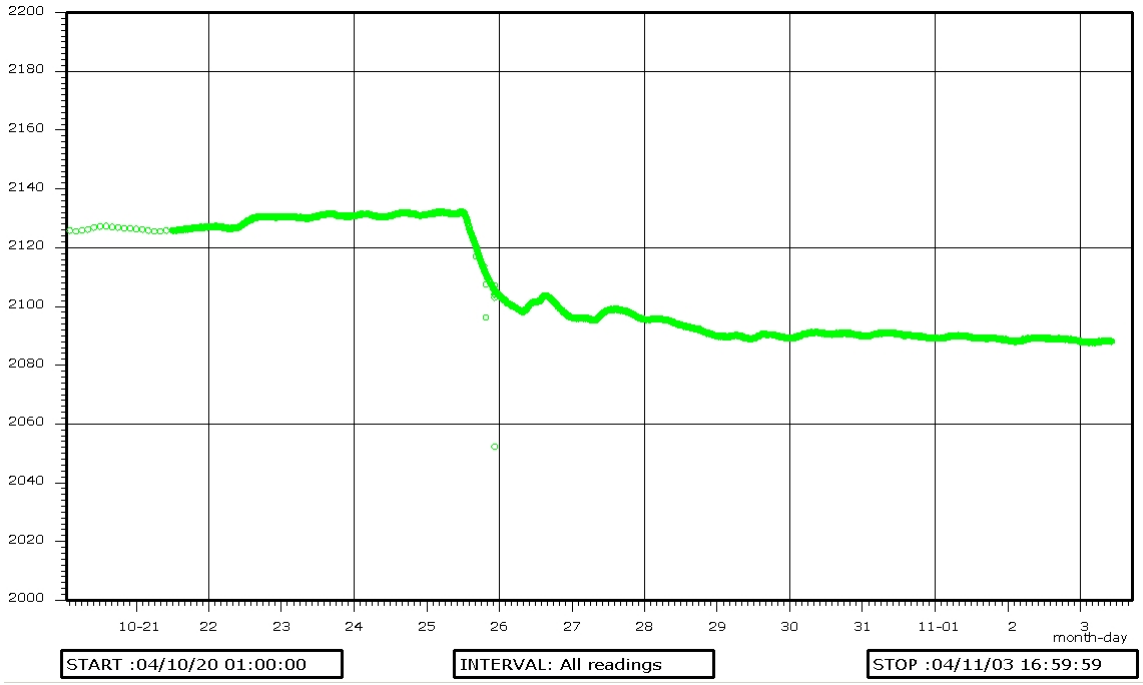

Figure 0-1. *Registered water pressure response (kPa) at borehole KA2598A during the period of the drilling of the de-stressing slot at the APSE site.*

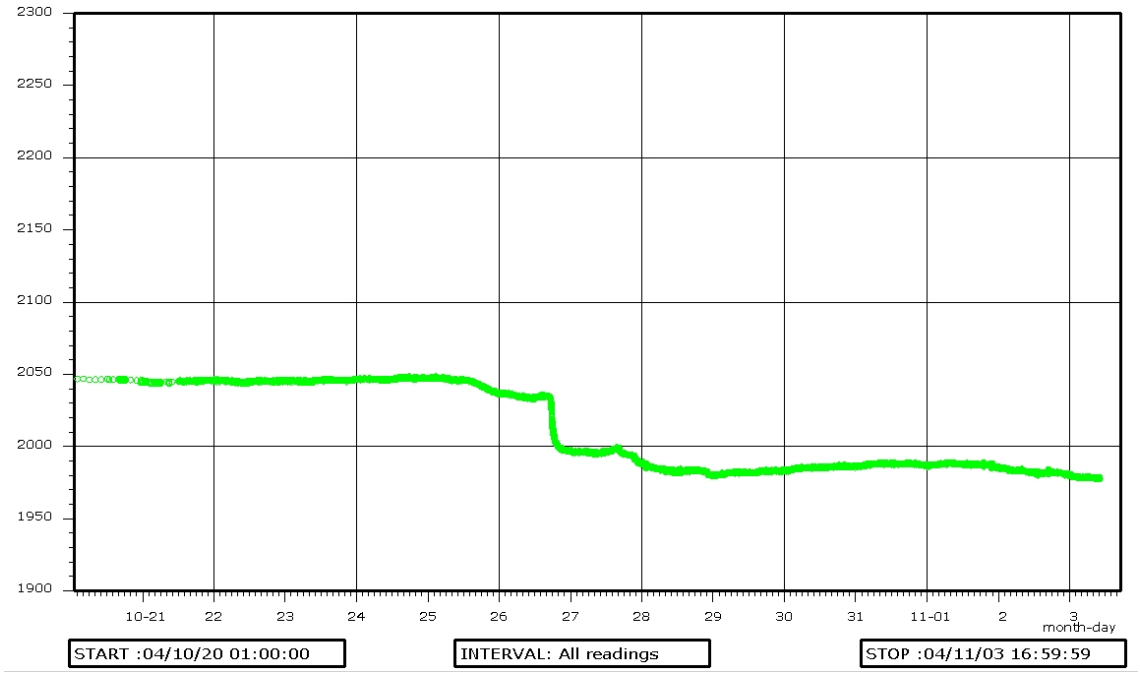

Figure 0-2. *Registered water pressure response (kPa) at borehole KA3386A01 during the period of the drilling of the de-stressing slot at the APSE site.*

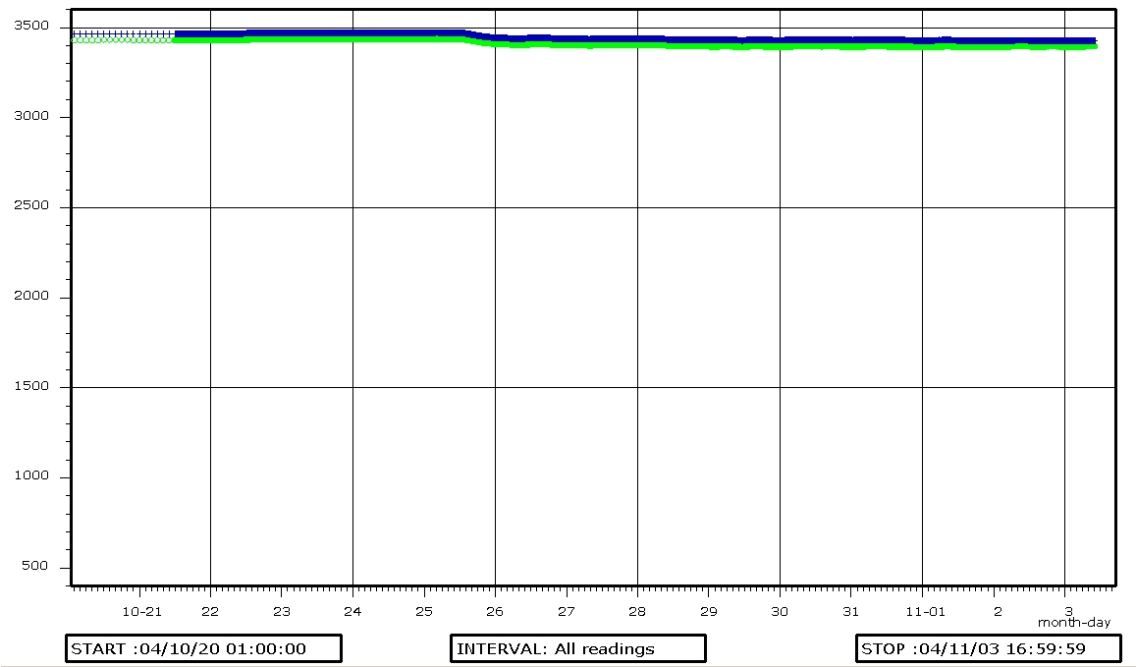

Figure 0-3. *Registered water pressure response (kPa) at borehole KA3385A during the period of the drilling of the de-stressing slot at the APSE site.*

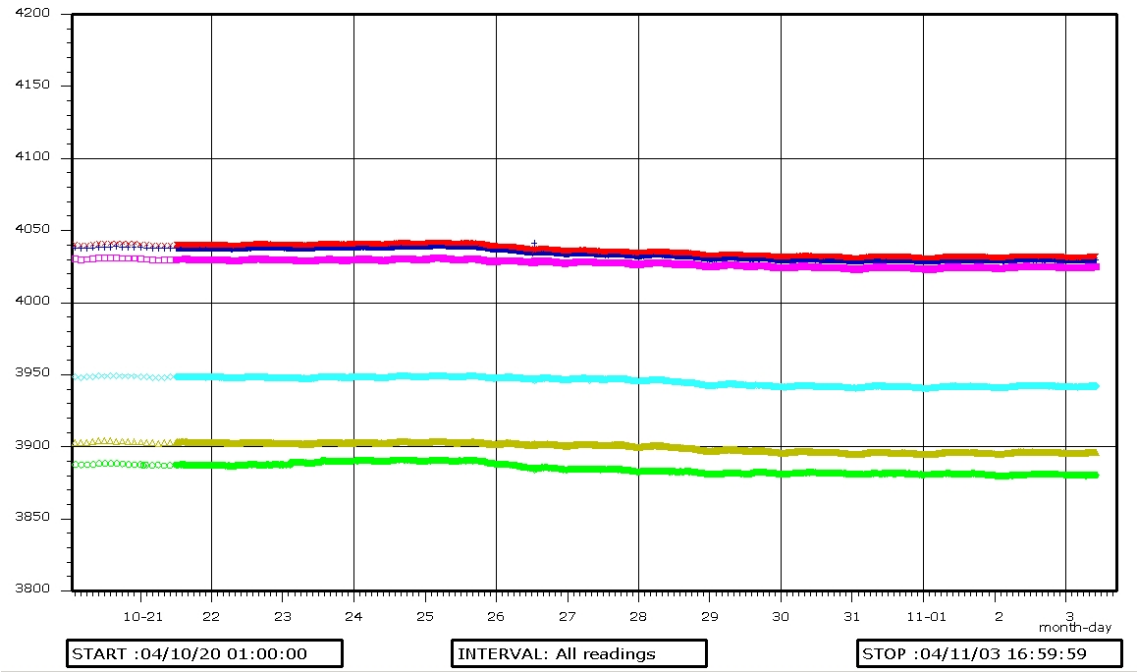

Figure 0-4. *Registered water pressure response (kPa) at borehole KI0025F during the period of the drilling of the de-stressing slot at the APSE site.*

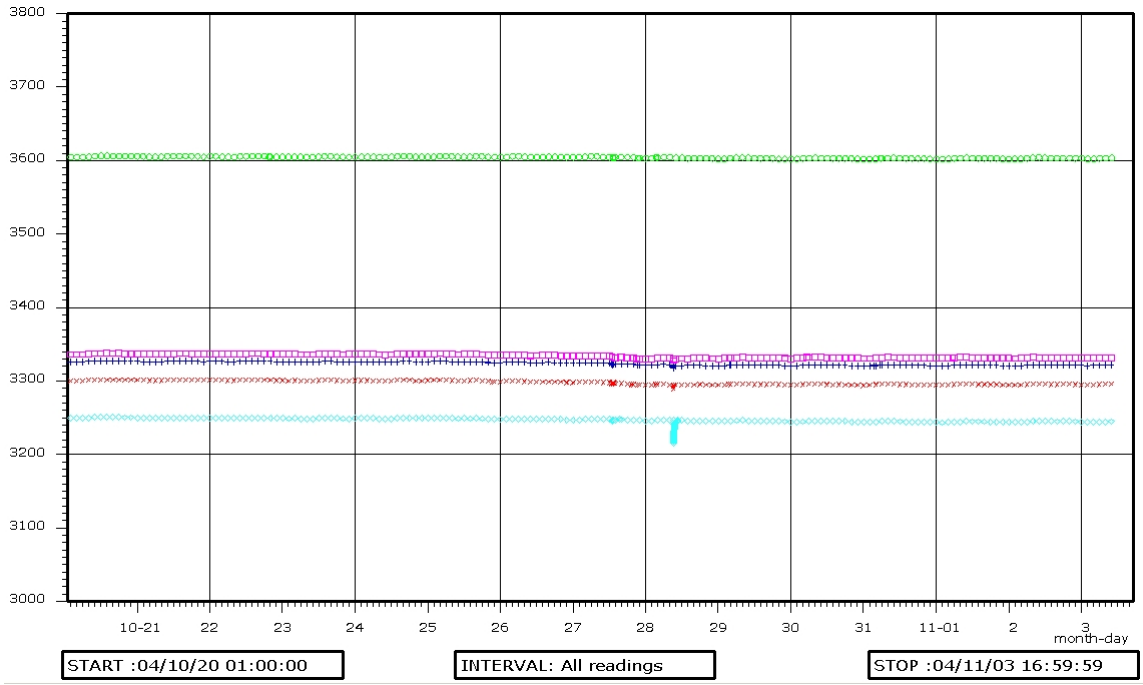

Figure 0-5. *Registered water pressure response (kPa) at borehole KA3105A during the period of the drilling of the de-stressing slot at the APSE site.*

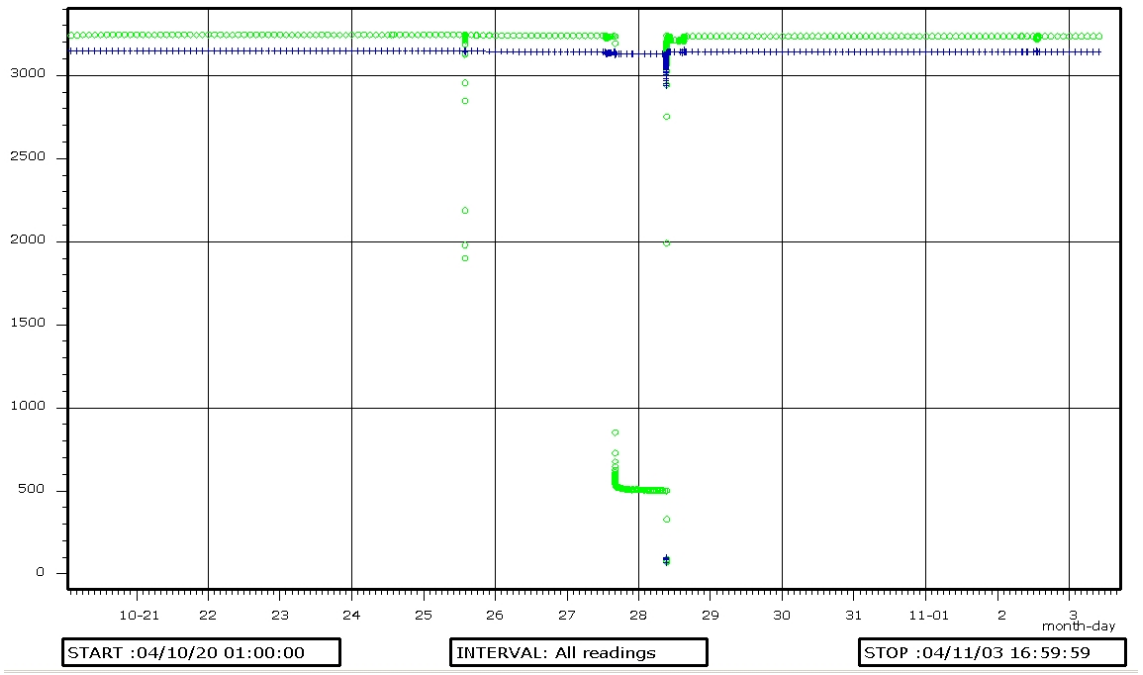

Figure 0-6. *Registered water pressure response (kPa) at borehole KA3110A during the period of the drilling of the de-stressing slot at the APSE site*

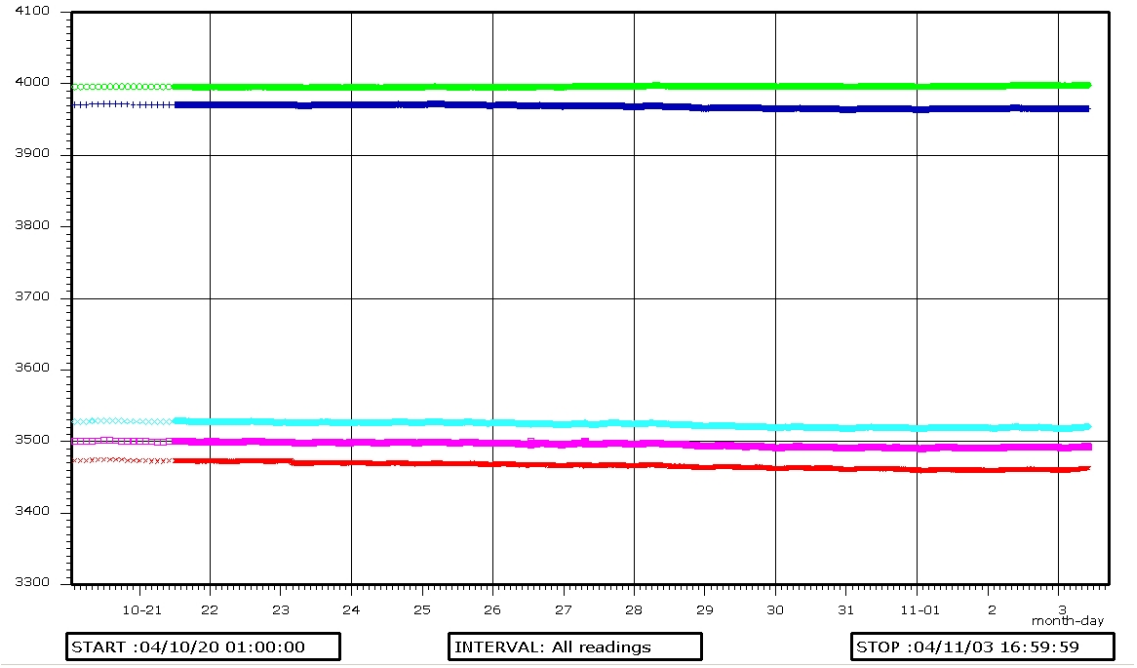

Figure 0-7. *Registered water pressure response (kPa) at borehole KA3510A during the period of the drilling of the de-stressing slot at the APSE site*

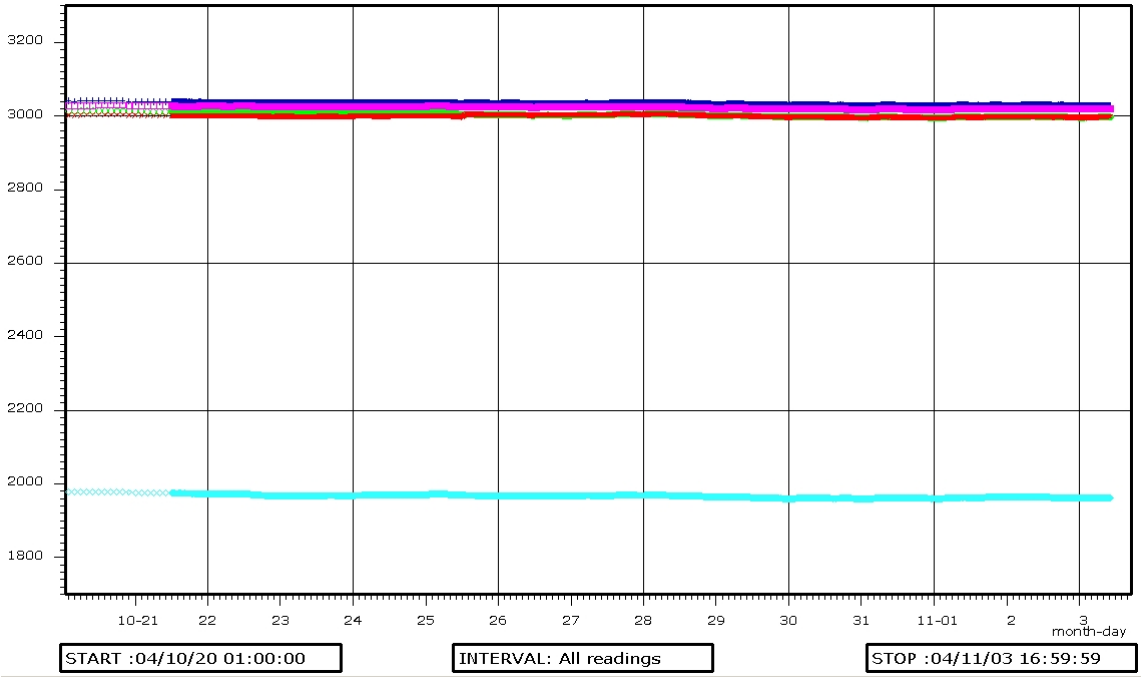

Figure 0-8. *Registered water pressure response (kPa) at borehole KG0021A01 during the period of the drilling of the de-stressing slot at the APSE site*

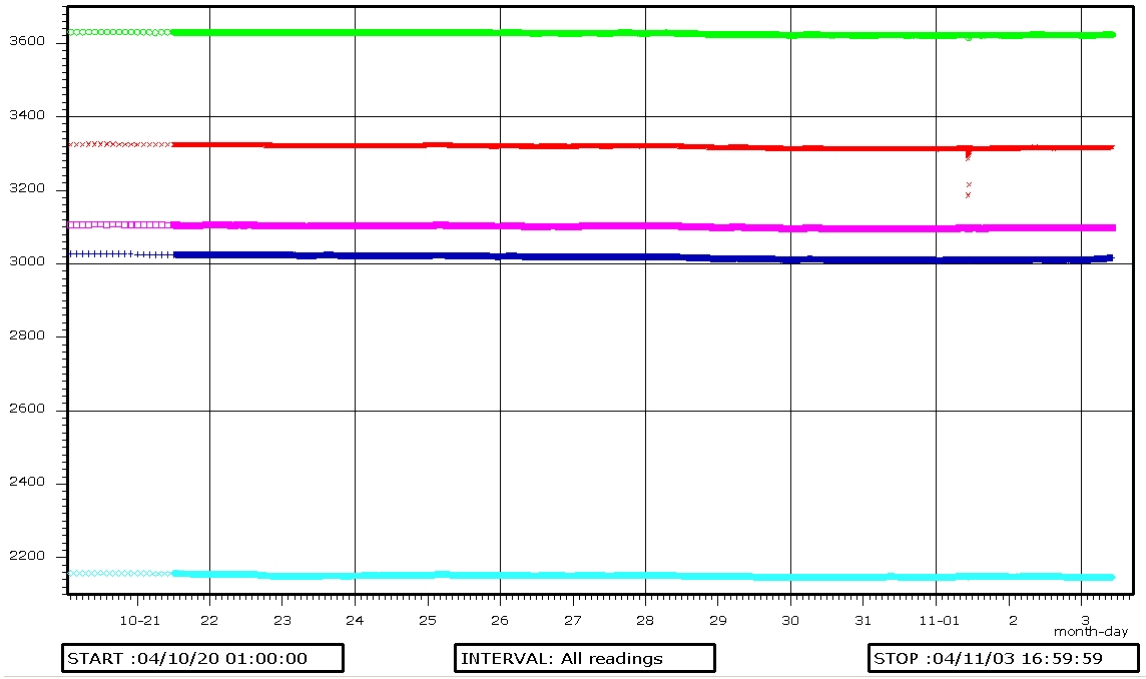

Figure 0-9. *Registered water pressure response (kPa) at borehole KG0048A01 during the period of the drilling of the de-stressing slot at the APSE site*

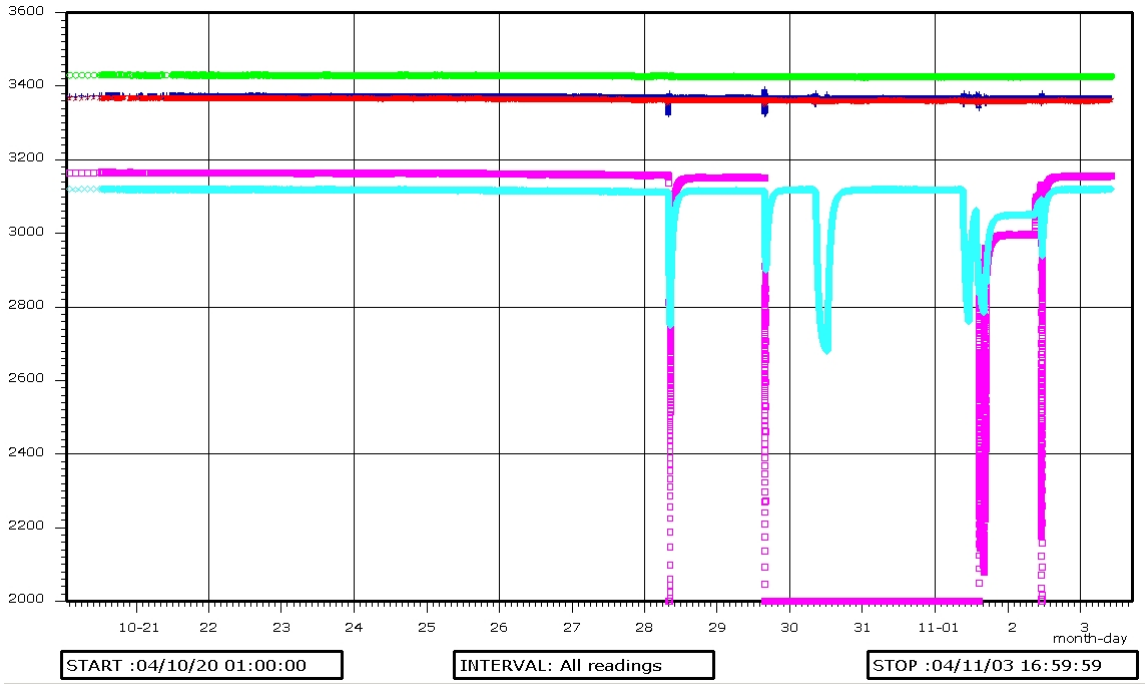

Figure 0-10. *Registered water pressure response (kPa) at borehole KXTT4 during the period of the drilling of the de-stressing slot at the APSE site*